CUSP SHAPES UNDER CONE DEFORMATION

Jessica S. Purcell

Abstract

A horospherical torus about a cusp of a hyperbolic manifold inherits a Euclidean similarity structure, called a cusp shape. We bound the change in cusp shape when the hyperbolic structure of the manifold is deformed via cone deformation preserving the cusp. The bounds are in terms of the change in structure in a neighborhood of the singular locus alone.

We then apply this result to provide information on the cusp shape of many hyperbolic knots, given only a diagram of the knot. Specifically, we show there is a universal constant C such that if a knot admits a prime, twist reduced diagram with at least C crossings per twist region, then the length of the second shortest curve on the cusp torus is bounded. The bound is linear in the number of twist regions of the diagram.

1. Introduction

1.1. Motivation. The interplay between geometry and topology is an important theme in the study of 3–manifolds. Since Thurston's work in the late 1970s, it has been known that any Haken 3–manifold has a geometric decomposition [**23**]. Recently, Perelman has announced a proof that any closed, orientable 3–manifold has such a decomposition (the geometrization conjecture). However, it is important not only to know the existence of a geometric structure on a 3–manifold, but also to understand the relation between that structure and the topological description of the manifold.

Often a 3–manifold is described topologically, for example by a combinatorial diagram indicating a knot complement in S^3, or a Dehn filling description (see Definition 1.1 below). However, relating this topological description to the geometry of the manifold seems to be very difficult, and remains an important problem in the area. There are few tools available to give geometric data from topological information. In this paper, we present a new such tool.

We are particularly interested in topological descriptions of 3–manifolds with torus boundary. These include all knot and link complements

in S^3, as well as knot and link complements in other 3–manifolds. It is a classic result due to Wallace and Lickorish that every closed, orientable 3–manifold is given by a Dehn filling on a link complement in S^3 ([**25**], [**18**]). Thus these manifolds are of fundamental importance in the subject.

We will also focus only on those manifolds which are hyperbolic. The link complements of Wallace and Lickorish above can be taken to be hyperbolic. Thurston showed that on any such cusped hyperbolic manifold "most" Dehn fillings are hyperbolic. That is, only a finite number of slopes per link component need be excluded; then any Dehn filling on remaining slopes yields a hyperbolic manifold [**23**]. Additionally, for knots in S^3, any knot that is not a torus or satellite knot is known to be hyperbolic [**24**]. Therefore, in some sense, most 3–manifolds are hyperbolic. Mostow–Prasad rigidity implies that the hyperbolic structure on these finite volume manifolds is unique [**19**], [**20**]. However, this unique structure is little understood.

Given a hyperbolic manifold with torus boundary components, i.e., given a *cusped* hyperbolic manifold, the geometric structure on the manifold allows us to associate a Euclidean similarity structure, called a cusp shape, to each boundary component. The cusp shapes of a manifold are geometric quantities which we will relate to a manifold's topological description.

There are several reasons one might be interested in knowing the cusp shape of a manifold. Cusp shape is an interesting piece of geometric information by itself. It also can be used to give a rough lower bound on the volume of the manifold, by calculating cusp volumes and using packing arguments such as those of Böröczky [**5**]. (See, however [**10**]: this lower bound may not be very sharp.) More importantly, knowing the cusp shape, we also obtain information on the geometry of manifolds obtained by Dehn filling. For example, we can find all filling slopes which might not yield a hyperbolic manifold [**3**], [**15**], [**14**].

Our main results give explicit bounds on the change in cusp shape of a 3–manifold with multiple cusps under all but finitely many Dehn fillings, where one cusp is left unfilled. This is essentially the content of Theorems 1.2, 1.3, and 1.4 below. The first, Theorem 1.2, is the most general, bounding cusp information. In Theorem 1.3, we give a differential inequality bounding the normalized lengths of curves on cusps. In Theorem 1.4, we bound the change in height of the cusp shape.

We also apply these results to the case of knots in S^3. Given only a diagram of a large class of knots, we are able to determine bounds on the height of cusps. This is the content of Theorem 1.8. Note that similar results, relating the geometry of a knot to its diagram, are rare. In fact, we know only of results relating volumes to a diagram. Lackenby found lower bounds on volumes of alternating knots based on a condition of

a diagram, and upper bounds for general knots [**16**]. The lower bounds were improved by Agol, Storm and Thurston [**4**], and the upper by Agol and D. Thurston in an appendix to Lackenby's paper [**16**]. Using cone deformations, we found similar bounds on volumes for another class of knots [**21**]. Using negatively curved metrics, we recently improved these results with Futer and Kalfagianni [**11**].

However, as far as we are aware, the results of this paper are the first of their kind giving actual geometric bounds on cusp shape based only on a diagram.

1.2. Cone deformations. Our primary technique is cone deformation, which we will now describe. Using properties of cone deformations, we obtain geometric information on the topological process of Dehn filling.

Definition 1.1. Given a manifold M with torus boundary ∂M and specified slope s on ∂M, we obtain a new manifold by gluing a solid torus to ∂M such that s bounds a disk in the solid torus. This is called the *Dehn filling of M along s*, or sometimes *Dehn surgery*, and the resulting manifold is denoted $M(s)$. More generally, if M has n torus boundary components with slopes $s_1, \ldots, s_n$, then we obtain $M(s_1, \ldots, s_n)$ in the same manner.

A geometric description of Dehn filling was investigated by Thurston [**23**]. Given a complete hyperbolic structure on a manifold M with torus boundary, he showed the structure could be deformed through incomplete hyperbolic structures with singularities at the core of the added solid torus to structures whose completion is again non-singular. These structures are exactly hyperbolic structures on Dehn filled manifolds $M(s)$. The space of deformations is called hyperbolic Dehn surgery space.

We restrict our attention to particular paths through hyperbolic Dehn surgery space in which the incomplete hyperbolic manifolds are all cone manifolds. That is, the completion gives a manifold with cone singularities along the core of the added solid torus, with cone angle α. (A more complete definition of a cone deformation is given in Definition 2.1 below.)

We have some control over cone deformations. Local rigidity results due to Hodgson and Kerckhoff [**13**], extended by Bromberg in the case of geometrically finite manifolds [**9**], give control on the change in geometry of the entire manifold, knowing only information on the change in a neighborhood of the singular locus.

This geometric control has been used recently to prove several interesting results in 3–manifold theory. Hodgson and Kerckhoff used it to give universal bounds on the number of exceptional Dehn surgery slopes for finite volume manifolds [**14**]. In the infinite volume case, cone deformations lie at the heart of drilling and grafting theorems, described

by Bromberg in [**8**]. These have recently been used to resolve problems in the field of Kleinian groups, such as the Bers density conjecture [**7**], and existence of type preserving sequences of Kleinian groups [**6**]. This paper gives another application of cone deformations, to finite volume manifolds with cusps.

1.3. Cusp shapes. Let M be a manifold admitting a hyperbolic structure, with a torus boundary component T. Under the hyperbolic structure on M, T will be a cusp. We take a horoball neighborhood of this cusp. Its boundary is a horospherical torus, which inherits a Euclidean structure from the hyperbolic structure on M. The structure is independent of choice of horoball neighborhood, up to scaling of the Euclidean metric. Thus we obtain a class of Euclidean similarity structures on T, which we call the *cusp shape* of the torus T.

Now, suppose the hyperbolic structure of M is changing under a cone deformation with singularities along a link Σ in M disjoint from T. Σ is called the singular locus of the deformation. T will remain a cusp throughout the deformation, and its cusp shape will be changing with the change of geometry of M. We bound this change in terms of the change in geometry in a neighborhood of Σ.

Theorem 1.2. *Suppose we have the following:*

- *M a complete finite volume hyperbolic 3–manifold with a cusp T.*
- *$X = X_0$ a complete finite volume hyperbolic 3–manifold which can be joined to $M = X_\tau$ by a smooth one–parameter family of hyperbolic cone manifolds X_t, such that cone angles go from 0 at time $t = 0$ to 2π at time τ.*
- *A singular locus, say with n components, such that the tube radius about each component is larger than $R_1 \geq 0.56$ for all t.*
- *A horoball neighborhood U_t of the cusp of X_t which deforms to T at time τ. Let $\gamma(t)$ denote the path ∂U_t travels through the Teichmüller space of the torus, endowed with Teichmüller metric $\|\cdot\|$.*

Then there exists a parameterization of the deformation such that we have the following bound for ∂U_t:

$$2\,\|\gamma'(t)\|^2 Area(\partial U_t) \leq n\,C(R_1).$$

Here $C(R_1)$ is a strictly decreasing function of R_1 which approaches 0 as R_1 approaches infinity. Moreover, we can assume $\tau \leq (2\pi)^2$.

Also interesting is the application of Theorem 1.2 to lengths of curves on the cusp in question. Let β be a slope on the cusp torus, and again let $\gamma(t)$ be the path that the cusp shape ∂U_t traces through the Teichmüller space of the torus. Let L_t be the normalized length of β under the deformation, with derivative $\dot{L} = \frac{d}{dt}L_t$ (see Section 3.3 for

more information). Then L_t will satisfy:

$$(1) \qquad\qquad -\|\gamma'(t)\|\, L_t \leq \dot{L} \leq \|\gamma'(t)\|\, L_t.$$

Combining equation (1) with the result of Theorem 1.2, we may bound the change in normalized length of a curve under a cone deformation.

Theorem 1.3. *Let the set up be as in Theorem* 1.2 *above. Let L_t be the normalized length of a slope on a cusp torus under the cone deformation, with derivative $\dot{L} = \frac{d}{dt} L_t$. Then there exists a parameterization of the cone deformation such that the change in L_t is bounded by the following inequality:*

$$-\left(\sqrt{\frac{n\, C(R_1)}{2\mathrm{Area}(\partial U_t)}}\right) L_t \leq \dot{L} \leq \left(\sqrt{\frac{n\, C(R_1)}{2\mathrm{Area}(\partial U_t)}}\right) L_t\ .$$

Finally, we use Theorem 1.3 to bound the normalized length of the arc perpendicular to the shortest curve on the cusp torus, and then bound the length of this shortest curve below. We then obtain an estimate that is independent of time.

Theorem 1.4. *Let the notation be as in Theorem* 1.2 *above. Denote by $h(M)$ the normalized* height *of the cusp torus ∂U_τ. That is, $h(M)$ is the normalized length of the arc perpendicular to the shortest curve on ∂U_τ that runs from the shortest curve back to the shortest curve (this arc might not be closed). Similarly, let $h(X)$ denote the normalized height of ∂U_0. Then there exists a parameterization of the cone deformation such that the change in normalized height is bounded in terms of R_1 alone:*

$$-(2\pi)^2 \frac{\sqrt{n\, C(R_1)}}{(1 - e^{-2R_1})\sqrt{2}} \leq h(M) - h(X) \leq (2\pi)^2 \frac{\sqrt{n\, C(R_1)}}{(1 - e^{-2R_1})\sqrt{2}}\ .$$

1.4. Applications to knot theory. In the last part of this paper we give specific applications of Theorem 1.4. We determine bounds on the cusp shape of a knot based solely on a diagram of that knot.

Before we state the results, we review some definitions.

Definition 1.5. Let $K \subset S^3$ be a knot with diagram $D(K)$. Define a *twist region* to be a region of $D(K)$ where two strands of the diagram twist around each other maximally. Precisely, if $D(K)$ is viewed as a 4–valent planar graph with over–under crossing information at each vertex, then a twist region is a maximal string of bigons in the complement of the graph arranged end to end, or a single vertex of the graph adjacent to no bigons.

We also require the diagram to be reduced, in the sense of the following two definitions. These definitions are illustrated elsewhere (see e.g., [**15**], [**12**]).

Definition 1.6. A diagram $D(K)$ is *prime* if when any simple closed curve γ intersects $D(K)$ transversely in two points in the interiors of edges, then γ bounds a subdiagram containing no crossings of the original diagram.

Definition 1.7. The diagram $D(K)$ is *twist reduced* if when any simple closed curve γ intersects $D(K)$ transversely in four points in the interiors of edges, with two of these points adjacent to one crossing and two others adjacent to another crossing, then γ bounds a subdiagram consisting of a (possibly empty) collection of bigons arranged end to end between these two crossings.

Any diagram of a prime knot or link can be simplified into a prime, twist reduced diagram. If the diagram is not prime, then crossings on one side of a simple closed curve are extraneous and can be removed. If the diagram is not twist reduced, then performing flypes will amalgamate two twist regions adjacent to a simple closed curve into one, reducing the number of twist regions.

For a hyperbolic knot complement, we can choose a horoball neighborhood about the cusp such that a meridian on the boundary of that horoball has length 1 (see e.g., [**2**]). Consider the geodesic arc orthogonal to the meridian which runs from meridian to meridian on this horospherical torus. Define the length of this arc to be the *height* of the cusp. Note that when the meridian is the shortest curve on the cusp (as will be the case in the knots of this paper), this definition of height agrees with that in Theorem 1.4.

Let K be a knot in S^3 which admits a prime, twist reduced diagram with at least 2 twist regions, with each twist region containing at least 6 crossings. Then it was shown in [**12**] that $S^3 - K$ is hyperbolic. The following theorem gives bounds on the cusp shape.

Theorem 1.8. *Let K be a knot in S^3 which admits a prime, twist reduced diagram with a total of $n \geq 2$ twist regions, with each twist region containing at least $c \geq 116$ crossings. In a hyperbolic structure on $S^3 - K$, take a horoball neighborhood U about K. Normalize so that the meridian on ∂U has length 1. Then the height H of the cusp of $S^3 - K$ satisfies:*

$$H \geq n \left(1 - f(c)\right)^2.$$

Here $f(c)$ is a positive function of c which approaches 0 as c increases to infinity.

Additionally, $H \leq n(\sqrt{n-1} + f(c))^2$.

The function f is given explicitly in Section 6. We can plug in values of c to obtain more specific estimates. For example, in Corollary 6.7 we let $c = 145$. Then $1 - f(c)$ is approximately 0.8154.

Note that the shortest non-meridional slope on the cusp of $S^3 - K$ will have length at least that of the height. So Theorem 1.8 implies that in this case, the shortest non-meridional slope has length at least $n (1 - f(c))^2$.

By results of Hodgson and Kerckhoff [**14**], Dehn filling along a slope with normalized length at least 7.515 results in a hyperbolic manifold. Corollary 6.7 implies that for a complicated knot, the shortest non-meridional slope will have normalized length at least $\sqrt{n}(0.8154)$. Thus the normalized length of a slope will be larger than 7.515 whenever $n \geq 85$. Thus we have the following corollary to Theorem 1.8:

Corollary 1.9. *Let K be a knot in S^3 which admits a prime, twist reduced diagram with at least 85 twist regions and at least 145 crossings per twist region. Then any non-trivial Dehn filling of $S^3 - K$ is hyperbolic.*

Corollary 1.9 is proven without any reference to the geometrization conjecture. If we assume that conjecture, then we recently proved (with Futer [**12**]) that the numbers 85 and 145 could be reduced to 4 and 6 respectively. However, note the proof of that result gives no geometric information on cusp geometry.

The numbers of crossings, 116 and 145, can be reduced significantly for certain classes of knots. We illustrate this in Section 6.4 for 2–bridge knots.

1.5. Organization of this paper. In Section 2, we review background information on cone deformations.

In Section 3, we begin the proofs of Theorems 1.2, 1.3, and 1.4 using information set up in Section 2. This leads us to results which contain certain boundary terms.

In Section 4, we give bounds on these boundary terms, which allow us to conclude the proof of Theorems 1.2 and 1.3.

We complete the proof of 1.4 in Section 5.

Finally, in Section 6 we apply the results of the previous sections to knots, and present the proof of Theorem 1.8.

2. Background on Cone Deformation

In this section, we will recall definitions associated with cone deformations and review relevant results from work of Hodgson and Kerckhoff ([**13**], [**14**]).

Definition 2.1. Let M be a 3–manifold containing a closed 1–manifold Σ. A *hyperbolic cone structure* on M is an incomplete hyperbolic structure on $X = M - \Sigma$, whose completion is singular along Σ. A cross section of a component of Σ is a hyperbolic cone with angle α, where α is constant along that component. (For a more complete description of the metric on M, see [**13**].) The set Σ is called the *singular locus* of M. M with this structure is called a *hyperbolic cone manifold*. A *hyperbolic cone deformation* on M is a smooth one–parameter family of hyperbolic cone structures X_t.

2.1. Infinitesimal deformations. Now, we may study deformations by considering possible "derivatives at time t" of X_t, or infinitesimal deformations of hyperbolic structure, for any time t. Each of these infinitesimal deformations corresponds to an element in a certain cohomology group $H^1(X; E)$, where recall $X = M - \Sigma$. We will be manipulating elements of $H^1(X; E)$, so we recall some information on their structure.

2.1.1. Cohomology. Given ω in $H^1(X; E)$, ω is a one–form on X with values in the vector bundle E of infinitesimal isometries of X. The bundle E has fiber $sl(2, \mathbb{C})$, which is the Lie algebra of infinitesimal isometries of $\mathbb{H}^3$. Recall that this Lie algebra has a complex structure. Geometrically, if s represents an infinitesimal translation in the direction of s, then is represents an infinitesimal rotation with axis in the direction of s. Thus on X we can identify E with the complexified tangent bundle $TX \otimes \mathbb{C}$, and write any $\omega \in H^1(X; E)$ in complex form: $\omega = v + iw$.

By the Hodge theorem proved in [**13**], in each cohomology class of $H^1(X; E)$ there is a *harmonic* representative of the form

$$\omega = \eta + i * D\eta,$$

where η is a unique TX-valued 1–form on $X = M - \Sigma$ that satisfies:

$$D^*\eta = 0,$$

(2) $$D^*D\eta + \eta = 0.$$

Here D is the exterior covariant derivative on such forms and D^* is its adjoint.

Thus we may assume that our cone deformation is chosen such that at each time t, the infinitesimal deformation of hyperbolic structure of X_t corresponds to a *harmonic* element ω in $H^1(X; E)$.

2.1.2. Tubular and Horoball neighborhoods. For purposes of this paper, we are particularly interested in the effect of the deformation in a neighborhood of the singular locus or in a horoball neighborhood of a cusp. So in this subsection, we will review a decomposition of ω (and η) into a nice form in these types of neighborhoods.

Select a component of the singular locus Σ of M. Let V be a tubular neighborhood of that component, with tube radius R. V is a solid torus with a singular core curve. During the cone deformation, the geometric structure on V is changing in meridional, longitudinal, and radial directions. We can write ω in V to reflect this:

$$(3) \qquad\qquad \omega = \omega_0 + \omega_c.$$

Here only $\omega_0 = \eta_0 + i * D\eta_0$ changes the holonomy of the meridian and longitude on the torus ∂V, and ω_c is a correction term.

We can further decompose ω_0 as follows:

$$(4) \qquad\qquad \omega_0 = u\,\omega_m + (x + iy)\,\omega_\ell.$$

Here, u, x, and y are real numbers. The 1–forms ω_m and ω_ℓ are standard forms, calculated in [**13**], which depend only on the tube radius R of V. The form $\omega_m = \eta_m + i * D\eta_m$ gives the change in the meridional direction. In particular, it represents the infinitesimal deformation which decreases the cone angle but doesn't change the real part of the complex length of the meridian. The form $\omega_\ell = \eta_\ell + i * D\eta_\ell$ stretches the singular locus, but leaves the holonomy of the meridian unchanged.

Since we will use the explicit formula for the standard form ω_ℓ in a calculation in a later section, we will restate that form here. Let e_1, e_2, and e_3 be an orthonormal frame for V in cylindrical coordinates, with e_1 pointing in the radial direction and e_2 tangent to the meridian. Let R be the radius of the tube V. Recall ω_ℓ is a $(TX \otimes \mathbb{C})$–valued 1–form, which can be viewed as an element of $Hom(TX, TX \otimes \mathbb{C})$. Thus it can be described as a matrix in the cylindrical coordinates e_1, e_2, e_3.

$$(5) \qquad \omega_\ell(R) = \begin{bmatrix} (\cosh R)^{-2} & 0 & 0 \\ 0 & -1 & -i\tanh R \\ 0 & -i\tanh R & 1 + (\cosh R)^{-2} \end{bmatrix}.$$

Now, so far, our decomposition of ω has been in a tubular neighborhood V of a component of the singular locus. We can do a similar decomposition of ω in a horoball neighborhood U of a cusp. In fact, we may consider U as a tubular neighborhood of a 1–dimensional submanifold of M on which the cone angle remains 0 throughout the deformation, and the tube radius is infinite. Again we may decompose ω as $\omega_0 + \omega_c$, where only ω_c affects the holonomy of the torus ∂U. But now, since the cone angle at the core of U is not changing, the meridional part of ω_0 is identically 0. Thus in this case,

$$\omega_0 = (x + iy)\,\omega_\ell,$$

where again x and y are real numbers, and ω_ℓ is a standard form. Since the tube radius of U is infinite, to write down the formula for ω_ℓ explicitly we let R go to infinity in equation (5).

$$(6) \qquad \omega_\ell(\infty) = \begin{bmatrix} 0 & 0 & 0 \\ 0 & -1 & -i \\ 0 & -i & 1 \end{bmatrix}.$$

2.2. Boundary terms. Our proof of Theorem 1.2 will involve certain boundary terms. In this section, we define these terms. We explain how they arise and recall certain properties. They will be used in the proof of Theorem 1.2.

Using results of the last section, we may always assume that we have a harmonic representative $\omega = \eta + i * D\eta$. Thus η satisfies equation (2).

Let N be any submanifold of $X = M - \Sigma$ with boundary ∂N oriented by the outward normal. When we take the L^2 inner product of equation (2) with η and integrate by parts over N, we obtain the boundary formula ([**14**, Lemma 2.3]):

$$(7) \qquad B(N) = \int_{\partial N} \eta \wedge *D\eta = \|\eta\|_N^2 + \| * D\eta\|_N^2$$

Here $\|\cdot\|$ denotes the L^2–norm on N. We will apply equation (7) to submanifolds of $X = M - \Sigma$ involving tubular or horoball neighborhoods.

First, we will introduce some notation. Let V_j be a tubular neighborhood of a component (the j-th component) of the singular locus, or a horoball neighborhood of a cusp. Using similar notation to that of [**14**], define

$$b_{V_j}(\zeta, \xi) = \int_{\partial V_j} *D\zeta \wedge \xi,$$

where ∂V_j is oriented such that the tangent vector orthogonal to ∂V_j is an outward normal when viewed from V_j. We will be considering $b_{V_j}(\eta, \eta)$ in this paper, and we review results concerning this term.

The decomposition (3) of ω in V_j into $\omega_0 + \omega_c$, and η into $\eta_0 + \eta_c$ decomposes the term $b_{V_j}(\eta, \eta)$:

$$(8) \qquad b_{V_j}(\eta, \eta) = b_{V_j}(\eta_0, \eta_0) + b_{V_j}(\eta_c, \eta_c).$$

That is, cross terms vanish ([**14**, Lemma 2.5]). Additionally, the term $b_{V_j}(\eta_c, \eta_c)$ is actually non-positive ([**14**, Lemma 2.6]), so we find

$$(9) \qquad b_{V_j}(\eta, \eta) \le b_{V_j}(\eta_0, \eta_0).$$

Now, let V be a tubular neighborhood of the entire singular locus Σ, as well as horoball neighborhoods of cusps. Thus V is a union of tubular neighborhoods V_j of components Σ_j of the singular locus and horoball

neighborhoods U_j. Then letting $N = X - V$ in equation (7),

$$(10) \quad B(X - V) \;=\; \|\eta\|_{X-V}^2 + \| * D\eta\|_{X-V}^2 = \int_{\partial V} *D\eta \wedge \eta$$

$$(11) \qquad\qquad\quad =\; \sum_j b_{V_j}(\eta, \eta) + \sum_k b_{U_j}(\eta, \eta).$$

The first sum is over all components of the singular locus, the second over all horoball neighborhoods of cusps. This equation, along with equation (9), implies

$$(12)\; 0 \le \sum_j b_{V_j}(\eta, \eta) + \sum_k b_{U_k}(\eta, \eta) \le \sum_j b_{V_j}(\eta_0, \eta_0) + \sum_k b_{U_k}(\eta_0, \eta_0).$$

Notice $\eta_0 = (\eta_0)_j$ depends on the neighborhood V_j or U_j. However, using the notation $b_{V_j}(\eta_0, \eta_0)$, it should be clear that we are referring to the decomposition of η particular to V_j in this context, and similarly for U_j. We will further simplify notation, using the following definition.

Definition 2.2. Let Σ_j be a component of the singular locus Σ. Let V_j be a tubular neighborhood of Σ_j of radius R. We let b_j be the boundary term:

$$b_j = b_{V_j}(\eta_0, \eta_0).$$

Remark. Note that for our applications of the results of this section, the one–form ω corresponds to an infinitesimal deformation of hyperbolic structure at time t. Thus ω, η, η_0, b_j, etc. will all depend on time t in our applications in future sections.

To avoid a notational nightmare, in the sequel we will assume the time t has been fixed, and continue writing these terms without reference to t, except occasionally where we feel recalling the dependency on t will help avoid confusion.

3. Change in Cusp Shape

In Section 2, we set up notation and reviewed known results. Given this information, we are ready to begin the proof of Theorem 1.2.

3.1. Boundary relations. Restrict to the case when we have a single cusp.

We will let U be a horoball neighborhood of the one cusp, and $V_1, \ldots, V_n$ be tubular neighborhoods of the components of the singular locus Σ, each with radius R. Here, we are letting n be the total number of components of Σ. We will assume throughout that these neighborhoods are chosen such that all intersections of distinct neighborhoods are trivial.

Let $\omega \in H^1(X; E)$ correspond to a harmonic infinitesimal deformation of hyperbolic structure at time t, and decompose ω in tubular

neighborhoods and horoball neighborhoods as in the previous section, and consider boundary terms.

By Equation (12), we see immediately that

$$(13) \qquad -b_U(\eta_0, \eta_0) \le \sum_{j=1}^{n} b_j.$$

Again, note that η_0 in the term $b_U(\eta_0, \eta_0)$ refers to the decomposition of η valid only in the horoball neighborhood U. Also, recall that the terms of equation (13) all depend on time t, but we are suppressing t for notational purposes.

Now, we will analyze the left hand side of (13). Recall that in a horoball neighborhood of a cusp, ω_0 can be written as a complex multiple of the form $\omega_\ell = \omega_\ell(\infty)$ in equation (6). That is, there are real numbers a and b (for fixed t) such that

$$(14) \qquad \omega_0 = (a + ib) \begin{bmatrix} 0 & 0 & 0 \\ 0 & -1 & -i \\ 0 & -i & 1 \end{bmatrix}.$$

Lemma 3.1. *Using the notation above,*

$$-b_U(\eta_0, \eta_0) = 2(a^2 + b^2)\,\mathrm{Area}\,(\partial U).$$

Proof. By Equation (14), we may write $\eta_0 = \mathrm{Re}(\omega_0)$ and $*D\eta_0 = \mathrm{Im}(\omega_0)$ as:

$$(15) \qquad \eta_0 = \begin{bmatrix} 0 & 0 & 0 \\ 0 & -a & b \\ 0 & b & a \end{bmatrix} = \begin{bmatrix} 0 \\ -a \\ b \end{bmatrix} \omega_2 + \begin{bmatrix} 0 \\ b \\ a \end{bmatrix} \omega_3$$

and:

$$*D\eta_0 = \begin{bmatrix} 0 & 0 & 0 \\ 0 & -b & -a \\ 0 & -a & b \end{bmatrix} = \begin{bmatrix} 0 \\ -b \\ a \end{bmatrix} \omega_2 + \begin{bmatrix} 0 \\ -a \\ b \end{bmatrix} \omega_3.$$

Here ω_1, ω_2, and ω_3 are forms dual to the vectors e_1, e_2, and e_3 giving cylindrical coordinates on U. Recall in particular that e_1 is radial, and e_2 is tangent to a meridian.

We then may compute $-b_U(\eta_0, \eta_0)$ explicitly in terms of the constants a and b:

$$-b_U(\eta_0, \eta_0) = \int_{\partial U} \eta_0 \wedge *D\eta_0 = \int_{\partial U} 2(a^2 + b^2)\omega_2 \wedge \omega_3.$$

Since $\omega_2 \wedge \omega_3$ is the area form for the torus ∂U, we have:

$$-b_U(\eta_0, \eta_0) = 2(a^2 + b^2)\mathrm{Area}(\partial U).$$

$$\text{q.e.d.}$$

Notice that Equation (13) and Lemma 3.1 imply:

$$0 \le \sum_j b_j, \tag{16}$$

and that we have equality by equation (11) if and only if η is trivial on $X - V$, which happens only when the deformation is trivial.

3.2. Teichmüller Space. We now turn our attention to the term $(a^2 + b^2)$ in Lemma 3.1. This term is closely related to the change in metric of the torus ∂U.

Under the hyperbolic metric on $X = M - \Sigma$, the boundary ∂U inherits a Euclidean structure. This gives a point in the Teichmüller space of the torus, $\mathcal{T}(T^2)$.

Remark. We view $\mathcal{T}(T^2)$ as the space of flat structures on the torus. To each flat structure ζ is associated a unit area Euclidean metric g_ζ, and vice versa. However, in the following discussion we will refer to both the flat structure and its associated metric, and so we will continue to distinguish between the two. We use Greek letters γ, ζ to denote points in $\mathcal{T}(T^2)$, and g with appropriate subscripts to denote the induced metric on the torus.

As the metric on X changes under the cone deformation, the point in $\mathcal{T}(T^2)$ will also change, tracing out a smooth path $\gamma(t)$, with tangent vector $\gamma'(t)$. The tangent vector $\gamma'(t)$ is an infinitesimal change of the flat structure on the torus. Our 1–form ω encodes the infinitesimal deformation of the hyperbolic cone structure X_t on $X = M - \Sigma$. So we may relate $\gamma'(t)$ to ω, or more particularly, to $a^2 + b^2$. We will do so using the Teichmüller metric on $\mathcal{T}(T^2)$.

Definitions of the Teichmüller distance vary by constant factors in the literature. We will use the convention that the Teichmüller distance between two points, σ and τ in $\mathcal{T}(T^2)$, is defined to be

$$d(\sigma, \tau) = \frac{1}{2} \inf_f \, \log K_f,$$

where $f \colon \sigma \to \tau$ is a K_f–quasiconformal map, with K_f the smallest such constant. (See for example [**17**].)

Lemma 3.2. *Let $\gamma(t)$ denote the path of ∂U through $\mathcal{T}(T^2)$. Let $\gamma'(t)$ denote its tangent vector. Then*

$$\sqrt{a^2 + b^2} = \left\| \gamma'(t) \right\|,$$

where the metric is the Teichmüller metric.

Proof. Fix $t = t_0$, and consider the flat structure on the torus given by $\partial U_{t_0} = \gamma(t_0)$. We may assume it has unit area. Recall that any Teichmüller geodesic through $\gamma(t_0)$ is given as follows. Select two orthogonal geodesic foliations F_1 and F_2 on the torus. Select $\lambda > 0$.

For any $u \in \mathbb{R}$, obtain a new metric by multiplying vectors along F_1 by $\exp(-\lambda\,u)$ and multiplying vectors along F_2 by $\exp(\lambda\,u)$. This is a "stretch–squeeze" map, which preserves the area of the torus. It gives a one–parameter family of flat structures on the torus, which we denote by $\zeta(u)$.

Teichmüller's theorem says that in the case of the torus, this stretch–squeeze map has the minimal quasiconformal distortion, so is a Teichmüller geodesic. For each u, the derivative of the map $\zeta(u)$ takes an infinitesimal circle to an infinitesimal ellipse, the ratio of whose axes is $\exp(2u\lambda)$. Thus for any u, the distance between the structure $\zeta(0) = \gamma(t_0)$ at time 0 and $\zeta(u)$ at time u is

$$d(\zeta(0), \zeta(u)) = \frac{1}{2} \inf_f \log K_f = \frac{1}{2} \log(e^{2u\lambda}) = \lambda\,u.$$

Therefore, $\lambda = \|\zeta'(u)\|$, where the norm is given with respect to the Teichmüller metric. In particular, $\lambda = \|\zeta'(0)\|$.

On the other hand, for any point on the torus, let u_1 and u_2 be orthonormal vectors in the directions of F_1 and F_2 respectively. Then when we write the infinitesimal change of metric induced by $\zeta'(0)$ in coordinates given by u_1 and u_2, we obtain at every point a diagonal matrix Λ with $-\lambda$, λ on the diagonal, since at each time u those vectors are just multiplied by $e^{-\lambda u}$, $e^{\lambda u}$, respectively. Thus if we let g_u be the metric on the torus induced by $\zeta(u)$, we have

$$\left.\frac{d}{du}\right|_{u=0} g_u(x, y) = 2g_0(\Lambda\,x, y).$$

Now we relate this discussion to the term $a^2 + b^2$.

Recall the infinitesimal deformation of the hyperbolic cone structure of X is encoded by the one–form ω. In particular, the infinitesimal change in metric is given by the real part η. That is, if we let g_t be the metric on X at time t, then

$$(17) \qquad\qquad \left.\frac{d}{dt}\right|_{t_0} g_t(x, y) = 2g_{t_0}(\eta(t_0)x, y).$$

(See the displayed equation on p. 374 of [**14**].)

We are interested in the infinitesimal change in the metric on ∂U_{t_0}. Since η decomposes into $\eta_0 + \eta_c$, and only η_0 changes the holonomy of ∂U, we know the infinitesimal change in metric on ∂U_{t_0} is given by η_0.

We have an explicit formula for η_0, written in orthonormal coordinates with respect to the metric g_{t_0}, given by e_1, e_2, e_3, where e_1 is radial and e_2 points in the direction of the meridian. Consider again equation (15). Since the first row and column for the matrix of η_0 are zero, we see that η_0 actually has no effect on or contribution to the change of metric in the radial direction of U. Hence, η_0 itself gives the infinitesimal change of metric on the torus ∂U_{t_0}, or $\gamma'(t_0) = \eta_0(t_0)$.

When we write η_0 in orthonormal coordinates e_2, e_3 on the torus, we discard the first row and column of the matrix of equation (15), and obtain the 2×2 matrix

(18)
$$A = \begin{bmatrix} -a & b \\ b & a \end{bmatrix}.$$

Here the first column of A gives the infinitesimal change in the meridional direction, the second the change in the direction orthogonal to the meridian. That is, if we restrict the metric g_t to ∂U_t, we may rewrite equation (17) as

$$\left. \frac{d}{dt} \right|_{t=t_0} g_t(x, y) = 2g_{t_0}(\eta_0(t_0)\, x, y) = 2 \langle Ax, y \rangle.$$

Hence A is a matrix representation of $\gamma'(t_0)$, the infinitesimal change of metric of the torus ∂U_{t_0}.

We can diagonalize A. For any point on the torus, there exist orthonormal vectors u_1 and u_2 such that when we put A into coordinates given by u_1 and u_2, A is diagonal with $-\sqrt{a^2 + b^2}$ and $\sqrt{a^2 + b^2}$ on the diagonal. Moreover, since A does not depend on the point on the torus (that is, for any point on the torus we obtain the same matrix A), u_1 and u_2 determine orthogonal geodesic foliations F_1 and F_2. These, in turn, determine a Teichmüller geodesic $\zeta(u)$ with $\zeta(0) = \gamma(t_0)$, whose initial tangent vector $\zeta'(0)$ agrees with A at every point, and has Teichmüller norm $\|\zeta'(0)\| = \sqrt{a^2 + b^2}$. Thus infinitesimally, $\gamma(t)$ and $\zeta(u)$ agree near $t = t_0$ and $u = 0$, respectively. Hence $\|\gamma'(t_0)\| = \|\zeta'(0)\| = \sqrt{a^2 + b^2}$. q.e.d.

Remark. In the proof of Lemma 3.2, we showed that for any time t, $\gamma(t)$ agrees infinitesimally with an explicit Teichmüller geodesic which is completely determined by the matrix A. We will use this again below.

Finally, putting Lemmas 3.1, and 3.2 together with Equation (13), we have completed the proof of the following theorem.

Theorem 3.3. *Let X_t be a hyperbolic cone deformation with a cusp. That is, for each time t, the hyperbolic cone manifold X_t has a cusp which remains a cusp throughout the deformation. Let U_t be a horoball neighborhood of the cusp. Let $\gamma(t)$ denote the path ∂U_t travels through the Teichmüller space of the torus. Then the change in ∂U_t is bounded by the following inequality:*

$$2 \|\gamma'(t)\|^2 \mathrm{Area}\,(\partial U_t) \leq \sum b_j(t).$$

The sum on the right hand side is over all components of the singular locus.

Note Theorem 3.3 gives an inequality identical to that of Theorem 1.2, except for the boundary terms b_j on the right hand side. We will

bound these, and complete the proof of Theorem 1.2, in Section 4. First, we set up a similar theorem to Theorem 1.3.

3.3. Normalized lengths on the torus. We are interested in determining how *normalized lengths* of curves on the torus ∂U change over the deformation.

Definition 3.4. Let β be a slope on the torus T, that is, an isotopy class of simple closed curves. The normalized length of β is defined to be:

$$\text{Normalized length}(\beta) = \frac{\text{Length}(\beta)}{\sqrt{\text{Area}(T)}},$$

where $\text{Length}(\beta)$ is defined to be the length of a geodesic representative of β on T.

Lemma 3.5. *Let β be a slope on ∂U_t. Let $L_t(\beta)$ denote its normalized length, with derivative $\dot{L}(\beta)$. Then $L_t(\beta)$ satisfies:*

(19) $$-\|\gamma'(t)\|\, L_t(\beta) \;\leq\; \dot{L}(\beta) \;\leq\; \|\gamma'(t)\|\, L_t(\beta).$$

Proof. Fix a time $t = t_0$. We will show the lemma for t_0.

We saw in the proof of Lemma 3.2 that $\gamma(t)$ agrees infinitesimally with an explicit Teichmüller geodesic $\zeta(u)$ determined by the matrix A of equation (18) when $t = t_0$ and $u = 0$. More specifically, $\zeta(u)$ multiplies vectors along F_1 by $\exp(-u\sqrt{a^2 + b^2})$, and multiplies vectors along F_2 by $\exp(u\sqrt{a^2 + b^2})$, where F_1 and F_2 are orthogonal geodesic foliations (determined by the matrix A) on the torus ∂U_{t_0}. Thus we will prove the lemma by showing it is true when the change in metric on ∂U_{t_0} is given by $\zeta(u)$.

Now, $L_t(\beta)$ is defined to be the length of a geodesic representative of β divided by $\sqrt{\text{Area}(\partial U_t)}$. Without loss of generality, we may assume that $\text{Area}(\partial U_t) = 1$, since $\gamma'(t)$ is given by a trace free (hence area preserving) matrix A. Thus $L_t(\beta)$ is just the length of a geodesic representative of β at time t_0.

Let $\hat{\beta}_{t_0} \colon I \to \partial U_{t_0}$ be a geodesic representative of β at time t_0. Then $\hat{\beta}_{t_0}$ makes some angle θ with the foliation F_1. For any u, $\zeta(u)$ takes $\hat{\beta}_{t_0}$ to a new geodesic, still with slope β, and length $L_u(\beta) = \alpha_u(\theta)\, L_{t_0}(\beta)$. Here

$$\alpha_u(\theta) = \sqrt{\cos^2\theta \, \exp(-2u\sqrt{a^2 + b^2}) + \sin^2\theta \, \exp(2u\sqrt{a^2 + b^2})}$$

is maximized when $\theta = \pi/2$ and minimized when $\theta = 0$. Thus we have

$$\exp(-\sqrt{a^2 + b^2}\, u)\, L_{t_0}(\beta) \leq L_u(\beta) \leq \exp(\sqrt{a^2 + b^2}\, u)\, L_{t_0}(\beta).$$

Since $\frac{d}{dt}\big|_{t=t_0} L_t(\beta) = \frac{d}{du}\big|_{u=0} L_u(\beta)$,

$$-\sqrt{a^2 + b^2}\, L_{t_0}(\beta) \leq \frac{d}{dt}\bigg|_{t=t_0} L_t(\beta) \leq \sqrt{a^2 + b^2}\, L_{t_0}(\beta).$$

q.e.d.

Combining this with the inequality of Theorem 3.3, we obtain the following theorem.

Theorem 3.6. *Let L_t be the normalized length of a slope on a cusp torus ∂U_t under a cone deformation, with derivative $\dot{L} = \frac{d}{dt} L_t$. Then the change in L_t is bounded by the following inequality:*

$$-\left(\sqrt{\frac{\sum b_i(t)}{2\,\mathrm{Area}\,(\partial U_t)}}\right) L_t \ \leq \ \dot{L} \ \leq \ \left(\sqrt{\frac{\sum b_i(t)}{2\,\mathrm{Area}\,(\partial U_t)}}\right) L_t.$$

Proof. Solving for $\|\gamma'(t)\|$ in the inequality of Theorem 3.3, we find

$$\|\gamma'(t)\| \leq \sqrt{\frac{\sum b_j(t)}{2\,\mathrm{Area}(\partial U_t)}}.$$

The result is given by substituting this into Equation (19). q.e.d.

3.3.1. Normalized height. For our applications, the curve on the torus we are particularly interested in is the one running orthogonal to the meridian. When we are dealing with link complements in S^3, as in a future section of this paper, there is a well defined meridian on a cusp torus. Otherwise, choose the shortest nontrivial simple closed curve on the initial cusp torus to be the meridian (for our applications to knots and links in S^3, these choices will agree).

We will be interested in estimating the length of the next shortest nontrivial simple closed curve. This length will be at least as long as the length of the arc orthogonal to the meridian.

At time t, let p_t denote the geodesic arc perpendicular to the meridian, running from meridian to meridian on ∂U_t. This arc will generally not be a closed curve. Let h_t be the normalized length of p_t, that is, $h_t = \mathrm{Length}(\mathrm{p_t})/\sqrt{\mathrm{Area}(\partial \mathrm{U_t})}$. We refer to h_t as the *normalized height* of the torus at time t. Denote its derivative at time t by $\dot{h}$.

Lemma 3.7. *The normalized height h_t satisfies*

$$-\sqrt{a^2 + b^2}\, h_t \leq \dot{h} \leq \sqrt{a^2 + b^2}\, h_t.$$

Proof. Let μ denote the meridian slope, with $L_t(\mu)$ its normalized length at time t. Then $h_t L_t(\mu) = 1$. Thus

$$\frac{\dot{h}}{h_t} + \frac{\dot{L}(\mu)}{L_t(\mu)} = 0.$$

By Lemma 3.5 and Lemma 3.2,

$$-\sqrt{a^2 + b^2} \le \frac{\dot{L}(\mu)}{L_t(\mu)} \le \sqrt{a^2 + b^2}.$$

Hence $-\sqrt{a^2 + b^2}\, h_t \le \dot{h} \le \sqrt{a^2 + b^2}\, h_t$.   q.e.d.

Again Lemma 3.7, combined with the inequality of Theorem 3.3, gives

$$(20) \qquad -\left(\sqrt{\frac{\sum b_i}{2\mathrm{Area}(\partial U_t)}}\right) h_t \le \dot{h} \le \left(\sqrt{\frac{\sum b_i}{2\mathrm{Area}(\partial U_t)}}\right) h_t.$$

We simplify equation (20) by noting the area of U_t is given by the length of the meridian times the actual length of the arc p_t. Recall that the length of p_t is $\sqrt{\mathrm{Area}(\partial U_t)}\, L_t(p_t) = \sqrt{\mathrm{Area}(\partial U_t)} h_t$. So denoting the length of the meridian of ∂U_t by m_t, we have

$$\sqrt{\mathrm{Area}(\partial U_t)} = m_t h_t.$$

Putting this into Equation (20), we obtain:

Theorem 3.8. *Let M be a hyperbolic 3–manifold with a cusp, and let X be a hyperbolic 3–manifold which can be joined to M by a smooth family of hyperbolic cone manifolds. Let h_t denote the normalized height at time t of the cusp which deforms to the cusp of M, and let m_t denote the length of its meridian. Finally, denote by $\dot{h}$ the derivative of h_t. Then*

$$(21) \qquad -\frac{\sqrt{\sum b_i(t)}}{m_t \sqrt{2}} \le \dot{h} \le \frac{\sqrt{\sum b_i(t)}}{m_t \sqrt{2}}.$$

4. Bounding the boundary terms

In this section, we finish the proofs of Theorems 1.2 and 1.3 by finding a parameterization of the cone deformation for which we may bound the sum $\sum b_j$.

In order to bound $\sum b_j$, we need more explicit formulas for the b_j. Recall that b_j was defined in Definition 2.2 as:

$$b_j = b_{V_j}(\eta_0, \eta_0).$$

Here η_0 is the real part of the 1–form ω_0 in the j-th component V_j of a tubular neighborhood of the singular locus. Thus we begin by revisiting our decomposition of ω_0 in V_j.

4.1. Convex combinations of deformations. Recall that corresponding to an infinitesimal deformation is the 1–form ω_0. We want ω_0 to have certain desired properties.

By Equation (4), we can decompose $\omega_0 = (\omega_0)_j$ in V_j as

$$(\omega_0)_j = u_j\,\omega_m + (x_j + iy_j)\,\omega_\ell,$$

with u_j, x_j, and y_j in $\mathbb{R}$, and where ω_m and ω_ℓ were computed in [**13**].

In [**14**], it was shown that if the singular locus has just one component, then the entire cone deformation can be parameterized by the square of the cone angle $t = \alpha^2$. In this case, $u = u_1$ was determined explicitly in [**14**]: $u = -1/(4\alpha^2)$, where α is the cone angle at the core of the singular solid torus $V = V_1$.

When we have multiple components of the singular locus, we may not necessarily be able to parameterize the cone deformation in this manner. However, we do have the following information.

First, for each j in $\{1,\ldots,n\}$, locally we have a deformation given by changing the j-th cone angle only and leaving the others fixed. This is a deformation with only one component of the singular locus, so the methods of [**14**] apply, and this deformation can be parameterized by $t = \alpha_j^2$. Then

$$(\omega_0)_j = -\frac{1}{4\alpha_j^2}\,\omega_m + (x_{jj} + iy_{jj})\omega_\ell.$$

Changing the angle in the j-th tube V_j and leaving the others fixed also affects the k-th tube V_k. Since there is no change of cone angle in this tube, $(\omega_0)_k$ can be expressed as

$$(\omega_0)_k = (x_{jk} + iy_{jk})\omega_\ell.$$

Any of these j deformations may be scaled by a factor $s_j \geq 0$, and we may take non-negative linear combinations. These correspond to new local deformations, in which the rates of change of cone angles vary according to the choice of the s_j. In a neighborhood of the j-th component, write:

$$(22) \qquad (\omega_0)_j = -\frac{s_j}{4\alpha_j^2}\,\omega_m + \sum_{k=1}^{n}(s_k x_{kj} + i\,s_k y_{kj})\,\omega_\ell.$$

Given a point $\bar{s} = (s_1, s_2, \ldots, s_n)$, we may use these equations for ω_0 to compute the forms η_0 explicitly, and thus compute the boundary terms $b_j = b_j(\bar{s})$ explicitly. Hodgson and Kerckhoff did the calculations without the extra $\bar{s}$ (p. 382 of [**14**]). When the $\bar{s}$ is put in, we obtain:

(23)

$$\frac{b_j(\bar{s})}{\text{Area}(\partial V_j)} = s_j^2\,c + \left(\left(\sum_k s_k x_{kj}\right)^2 + \left(\sum_k s_k y_{kj}\right)^2\right)a + s_j\left(\sum_k s_k x_{kj}\right)b.$$

Here the terms a, b, and c are constants in terms of R which agree with those on p. 383 of [**14**]. However, we are not immediately concerned with their values. More importantly, a is always negative, b and c always positive.

From the formula (23) we obtain the following information.

1) $b_j(\bar{s})$ is quadratic in $\bar{s}$.

2) If any $s_j = 0$ for some $\bar{s}$, then $b_j(\bar{s}) \leq 0$.

We also know that the sum of all the b_j's is strictly positive, provided $\bar{s} \neq (0, 0, \ldots, 0)$, by equation (16), as well as the remark right after that equation. We will use this information in §4.2.

4.2. Selecting local deformations. Each choice of $\bar{s} = (s_1, \ldots, s_n)$ corresponds to a local deformation with 1–form $(\omega_0)_j$ expressed in V_j as in equation (22). In terms of the deformation, varying $\bar{s}$ varies the rates at which the cone angles are changing (instantaneously). When $\bar{s} = (1, \ldots, 1)$, all cone angles are changing at the same rate. It might be convenient to let $\bar{s} = (1, \ldots, 1)$, to simplify calculations. However, such a choice may not give us the bounds on $\sum b_j$ that we need.

In particular, we would like to select $\bar{s}$ such that we may use certain inequalities from [**14**]. (These inequalities appear in the proof of Lemma 4.3 in this paper.) In order to use these inequalities, we will need to find $\bar{s}$ such that each $b_j(\bar{s}) \geq 0$.

The existence of such an $\bar{s}$ has been discovered by Hodgson and Kerckhoff, but their result is unpublished, so we include it as Lemma 4.1 here.

Lemma 4.1 (Hodgson–Kerckhoff). *There is an $\bar{s} \neq 0$ for which $b_j(\bar{s}) \geq 0$ for all $j = 1, 2, \ldots, n$.*

Proof. It suffices, by rescaling, to restrict $\bar{s}$ to the simplex

$$T = \{\bar{s} = (s_1, \ldots, s_n) | \sum_j s_j = n, s_j \geq 0\}.$$

We first set up some notation.

Let the j-th vertex of T be denoted t_j. So $t_j = (0, \ldots, 0, n, 0, \ldots, 0)$ where the single non-zero value is in the j-th location. Notice that at t_j, $b_i(t_j) \leq 0$ for all $i \neq j$. Because the sum of the b_i is always strictly positive, we must have $b_j(t_j) > 0$.

Let the face of T opposite t_j be denoted f_j. That is, on f_j the j-th coordinate is always 0. Notice that on f_j, $b_j \leq 0$. We will assume that $b_j < 0$ on f_j. If not, consider instead level sets of b_j for values $\epsilon > 0$ arbitrarily close to 0. Below, we will be finding points where all the b_j are positive. Taking a limit will at least give points where the b_j are nonnegative.

We will also assume level sets $b_j = 0$ intersect transversely. If not, take an arbitrarily small perturbation of the quadratic functions (keeping them quadratic).

First, we note that the set where $b_j > 0$ is an open neighborhood of t_j in T. This is because on any line from t_j to f_j, b_j goes from positive to negative. Because $b_j(s)$ is quadratic in s, $b_j = 0$ on this line in exactly one value. Thus the level set $b_j = 0$ separates t_j from f_j. It has a well–defined positive and negative side.

Now, we prove the following sublemma by induction:

Lemma 4.2. *Consider the $k - 1$ simplex S_k of T where $s_i = 0$ for all $i > k$. There exists a nonempty open set $B_k \subseteq S_k$ where $b_j > 0$ for all $j \leq k$. Furthermore, the set $E_k \subseteq S_k$ where $b_j = 0$ for all $j < k$ is an odd number of points, each on the boundary of B_k.*

Notice that in the above statement, when $k = n$, the simplex S_n is all of T. Then if the statement is true, B_n is an open set on which all the b_j are positive, so this will prove Lemma 4.1.

An additional fact we will pick up from the proof is that the set E_n where $b_j = 0$ for $j = 1, 2, \ldots, n - 1$ is an odd number of points. (We will use this additional fact in the proof of Lemma 4.4 below.)

Proof. We first prove Lemma 4.2 when $k = 2$. In this case, S_2 is the 1–simplex from t_1 to t_2. At t_1, $b_1 > 0$. At t_2, $b_1 < 0$. Since b_1 is quadratic, somewhere on S_2 is a single point e_2 where $b_1 = 0$. Notice that $b_2(e_2)$ must be positive. This is because each $b_j(e_2) \leq 0$ for $j > 2$ (since the corresponding coordinates s_j are all zero). Since $b_1(e_2)$ is zero, and the sum $\sum b_i > 0$, this forces $b_2 > 0$. Then in this case, E_2 contains the single point e_2. B_2 is nonempty, with e_2 on its boundary.
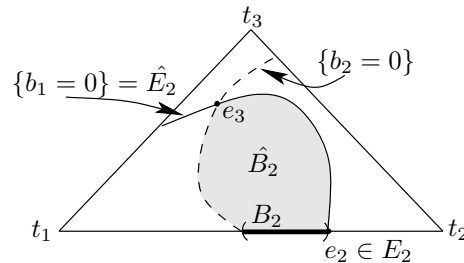

Figure 1. Proof of Lemma 4.1 when $k = 3$.

We will now prove the lemma by induction for $k + 1$. For reference, an example of the case when $k + 1 = 3$ is illustrated in Figure 1.

S_{k+1} is the k subsimplex of T with vertices $t_1, t_2, \ldots, t_{k+1}$, on which $s_{k+2} = \cdots = s_n = 0$. It has as one boundary face the $k - 1$ simplex S_k, on which $s_{k+1} = s_{k+2} = \cdots = s_n = 0$. On any other face of S_{k+1}, $s_{k+2} = \cdots = s_n = 0$, and also $s_j = 0$ for some $j < k + 1$.

By induction, we are assuming that on the face S_k the set B_k, where $b_j > 0$ for all $j \leq k$, is a nonempty open set. By continuity, the set

$\hat{B}_k$ in S_{k+1} where the same $b_j > 0$ must also be nonempty. The set $\hat{E}_k \subset S_{k+1}$ where $b_j = 0$ for $j < k$ is a 1–manifold with boundary. A neighborhood of E_k in $\hat{E}_k$ lies in the boundary of $\hat{B}_k$.

Consider $\hat{E}_k$. As a 1–manifold, it consists of closed components and arcs. The part of its boundary contained in S_k is the set E_k, so it consists of an odd number of points. Hence there must be an odd number of arc components of $\hat{E}_k$ with exactly one endpoint in S_k.

Consider the other boundary components of $\hat{E}_k$. They must lie on faces of S_{k+1}. Recall the set $\{b_j = 0\}$ does not intersect any face f_j where $s_j = 0$. Thus the only possible additional face of intersection of $\hat{E}_k$ and S_{k+1} is the face on which $s_k = s_{k+2} = \cdots = s_n = 0$, spanned by vertices $t_1, \ldots, t_{k-1}$ and t_{k+1} (note this face is in f_k). By induction (using the induction hypothesis with vertices renumbered), there are an odd number of intersection points of $\hat{E}_k$ on this face of S_{k+1}.

Thus there must be an odd number of arcs of $\hat{E}_k$ running from S_k to the face f_k. Along any of these arcs, b_k goes from positive (at a point of E_k on S_k) to negative (since $b_k < 0$ on f_k). Thus it must be zero at an odd number of interior points. Each of these points is in E_{k+1}. We may also have points of E_{k+1} coming from the intersection of $\{b_k = 0\}$ with closed components of $\hat{E}_k$, or with arc components of $\hat{E}_k$ with both endpoints of the arc on the same face (either S_k or f_k). In the former case, $\{b_k = 0\}$ must intersect any closed component an even number of times, and in the latter case b_k has the same sign on both endpoints, so again $\{b_k = 0\}$ intersects the arc an even number of times. Thus the total number of points in E_{k+1} is odd.

At each point in E_{k+1}, we have $b_1 = b_2 = \cdots = b_k = 0$, and we have b_{k+2} through b_n all less than or equal to zero. Since the sum of all the b_j is positive, b_{k+1} must be positive. This implies B_{k+1} is a nonempty open set, and the points of E_{k+1} are on its boundary.   q.e.d.

This completes the proof of Lemma 4.1.   q.e.d.

Now, as mentioned above, the choice of $\bar{s}$ is tied to the rates at which the cone angles are varying. Lemma 4.1 implies that a desired $\bar{s}$ exists, but gives us no further information about $\bar{s}$. In particular, some cone angle may reach 2π before the others. When this happens, the hyperbolic structure in the corresponding tube about the singular locus is nonsingular. We may thus view the deformation from this point on as a deformation on a cone manifold with one fewer component of the singular locus. We do this, obtaining deformations with fewer and fewer singular components, until each cone angle has reached 2π.

4.3. Boundary bound. In this subsection, we will show that there exists a parameterization of the cone deformation such that the sum of the terms b_j is of order n. We first need two lemmas. Lemma 4.3 gives

us an initial bound on each b_j. Lemma 4.4 will allow us to improve this bound. It is in the proof of Lemma 4.3, giving the initial bounds on the b_j, that we use the positivity result of Lemma 4.1.

Finally, in Theorem 4.6 at the end of this subsection, we put these lemmas together to record the main result of the section: the bound on the sum $\sum b_j$.

Lemma 4.3. *Suppose we have a cone deformation given as a linear combination of deformations, as above, where cone angles go from 0 to 2π along the singular locus. Suppose also that $S = (s_1, \ldots, s_n)$ is chosen such that for each time t, $b_j(S) \geq 0$ for all j. Suppose the tube radius R is bounded below by $R_1 \geq 0.56$ for each t. Then*

$$b_j(S) \leq s_j^2 \, C(R_1),$$

where $C(R_1)$ is a function of R_1 alone which approaches 0 as R_1 approaches infinity.

Proof. First, since we're considering a fixed V_j, we will drop the subscript j in our notation throughout the proof (i.e., $V_j = V$, $(\eta_0)_j = \eta_0$, $s_j = s$, etc).

Modify a calculation (p. 382 and 383 of [**14**]) to include s, and equation (17) of that paper can be written:

$$\frac{b_j(S)}{\text{Area}(\partial V)} \leq \frac{s^2}{8m^4},$$

where $m = \alpha \sinh^2 R$ is the length of a meridian on ∂U.

We will bound the term $\text{Area}(\partial V) \, s^2/(8m^4)$.

Let $A = \text{Area}(\partial V)$. Let h denote the height of ∂V, i.e., the length of an arc perpendicular to the meridian. So $h = \ell \cosh R$, where ℓ is the length of the singular locus of the solid torus V, and $A = mh$.

Consider

$$\Phi = \frac{8m^4}{A} = \frac{8m^3}{h} = \frac{8\alpha^3 \sinh^3 R}{\ell \cosh R}.$$

We will bound Φ below, therefore bounding its reciprocal above.

Let

$$\Upsilon(R) = \frac{3.3957 \tanh R}{2 \cosh 2R}.$$

It was shown in [**14**] (see Theorem 4.4, Corollary 5.1, and the comments on the multicusp case on p. 411), that $\alpha \ell \geq \Upsilon(R)$.

Then

$$\Phi = \frac{8\alpha^3 \sinh^3 R}{\ell \cosh R} = \frac{4\alpha^3}{\ell} \frac{1}{\Upsilon(R)} g(R)$$

where

$$g(R) = \frac{2\Upsilon(R) \sinh^3 R}{\cosh R} = 2\Upsilon(R) \tanh R \sinh^2 R = \frac{3.3957 \tanh^4 R}{1 + \tanh^2 R}.$$

So

$$\Phi \geq \frac{4\alpha^3}{\ell}\frac{1}{\alpha\ell}g(R) = 4\left(\frac{\alpha}{\ell}\right)^2 g(R).$$

Note that $g(R)$ is increasing with R. Hence since $R \geq R_1$, $g(R)$ is bounded below by $g(R_1)$. Thus we focus on the term α/ℓ in Φ.

Define $u = \alpha/\ell$. In our hyperbolic cone deformation, the initial cone angle α is zero. As α approaches 0, u approaches L_0^2, where L_0 is the normalized length of the curve which becomes the meridian (i.e., bounds a singular solid disc) under the cone deformation (see equation (37) of [14]). We will estimate $u = (u_0 + \Delta u) = (L_0^2 + \Delta u)$.

Reworking the calculations of [14] to include the speed s, and taking derivatives with respect to cone angle α rather than time, we may rewrite Proposition 5.6 of that paper as:

$$\frac{1}{\alpha}\frac{du}{d\alpha} \geq -\frac{2(1 + \tanh^2 R)}{3.3957\tanh^3 R} = -\frac{2\tanh R}{g(R)},$$

provided that $R \geq R_1 \geq 0.531$.

It is at this step, to use Proposition 5.6 of [14], that we have required S to be chosen so that $b_j(S) > 0$.

Thus

$$\Delta u \geq \int_{\alpha=0}^{\alpha=2\pi} -2\alpha\frac{\tanh R}{g(R)}d\alpha \geq -\frac{\tanh R_1}{g(R_1)}\int_0^{2\pi}2\alpha d\alpha = -(2\pi)^2\frac{\tanh R_1}{g(R_1)}.$$

So

$$u^2 \geq (L_0^2 - (2\pi)^2\tanh(R_1)/g(R_1))^2,$$

provided the term $L_0^2 - (2\pi)^2\tanh(R_1)/g(R_1)$ is non–negative. We can ensure this quantity is non–negative by ensuring L_0^2 is large. This can be done following [14]. The following result is essentially Equation (47) of that paper.

$$(24) \qquad L_0^2 \geq \frac{2(2\pi)^2}{3.3957(1 - \tanh R)}\exp\left(\int_1^{\tanh R}F(w)dw\right) = I(R),$$

provided the tube radius is at least R throughout the deformation. Here $F(w) = -(1+4w+6w^2+w^4)/((w+1)(1+w^2)^2)$ is an integrable function.

The right hand side $I(R)$ of (24) is increasing with R, so it can be bounded below by a constant in terms of R_1.

$$L_0^2 \geq I(R_1).$$

Now if $R_1 \geq 0.56$, then $I(R_1) - 2(2\pi)^2\tanh(R_1)/g(R_1) \geq 0$.

Putting this together,

$$\Phi \geq 4\left(I(R_1) - (2\pi)^2\frac{\tanh R_1}{g(R_1)}\right)^2 g(R_1).$$

The right hand side of the above equation is a constant, $\widetilde{C}_0(R_1)$.

Thus we have

$$b_j(S) \leq \frac{A}{8m^4} \, s^2 = \frac{1}{\Phi} \, s^2 \leq \frac{s^2}{\widetilde{C}_0(R_1)} = s^2 \, C(R_1).$$

<div align="right">q.e.d.</div>

The result of Lemma 4.3 gives us a bound on the sum of the b_j in terms of $\bar{s}$. If we could choose $\bar{s} = (1, \ldots, 1)$ (all cone angles increasing at the same rate), then Lemma 4.3 would give a bound on $\sum b_j$ of order n. However, our choice of $\bar{s}$ comes from Lemma 4.1. By the proof of that lemma, we may assume only that $\bar{s}$ is in the simplex $T = \{\bar{s} \,|\, \sum s_j = n, s_j \geq 0\}$. A priori, $\bar{s}$ could be close to a vertex of T, say $(n, 0, \ldots, 0)$, in which case Lemma 4.3 gives only a bound of order n^2 on $\sum b_j$.

For our applications, we need the bound of order n. We will obtain this better estimate by again revisiting the choice of the point $\bar{s} = (s_1, s_2, \ldots, s_n)$. This is done in Lemma 4.4.

Lemma 4.4. *There exists a point $S = (s_1, \ldots, s_n)$ in T such that each $b_j(S) \geq 0$, $j = 1, \ldots, n$, and for any index j with $s_j \neq \min\{s_1, \ldots, s_n\}$, we have $b_j(S) = 0$.*

Proof. First, we set up some notation.

Notation. Let $B = \{\bar{s} \,|\, b_j(\bar{s}) \geq 0, j = 1, \ldots, n\}$ (so the interior of B is the set B_n of Lemma 4.2). Again we may normalize such that the points $\bar{s}$ lie in the simplex $T = \{(s_1, \ldots, s_n) \,|\, \sum s_i = n, s_i \geq 0\}$.

We define some sets in B. For each $j = 1, 2, \ldots, n$, let e_j be the set of all points in B such that $b_j > 0$ and for $i \neq j$, $b_i = 0$. Note for $j = n$, e_n corresponds to the set E_n in Lemma 4.2. (So in particular, e_n consists of an odd number of points.)

Let $b_{\{i,j\}}$ be the set $b_{\{i,j\}} = B \cap (\cap_{k \neq i,j} \{b_k = 0\})$. Note $b_{\{i,j\}}$ has dimension 1, with components with boundary in e_i and e_j.

In general, let I be a k-element subset $I = \{i_1, i_2, \ldots, i_k\} \subseteq \{1, \ldots, n\}$. Let $b_I = B \cap (\cap_{j \notin I} \{b_j = 0\})$. Notice b_I is bounded by components b_{I_j} where $j \in I$, and I_j is the $(k-1)$-element set obtained by removing j from I.

Now we define some sets in the simplex $T = \{\bar{s} \,|\, \sum s_i = n\}$. Let T_i be the region in which $s_i \leq s_j$ for all indices j. T_i has dimension $n-1$. Let $T_{\{i,j\}} = T_i \cap T_j$. Thus each T_i is bounded by faces $T_{\{i,j\}}$ where j ranges over all elements of $\{1, \ldots, n\} - \{i\}$, as well as faces on ∂T. Generally, let I be a k-element subset of $\{1, \ldots, n\}$. Let $T_I = \cap_{j \in I} T_j$. Note the boundary faces of T_I are the faces given by $T_{I \cup \{k\}}$, where k ranges over all elements of $\{1, \ldots, n\} - I$, as well as faces in ∂T. See Figure 2 for an illustration when $n = 3$.
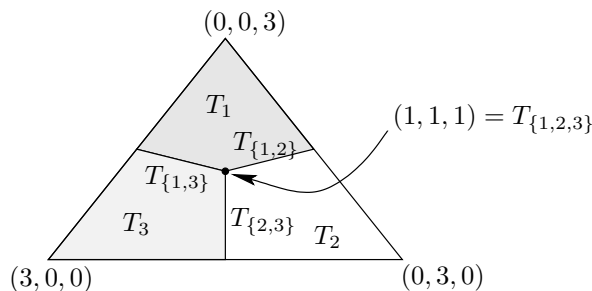
Figure 2. Faces T_I illustrated when $n = 3$.

We will make transversality assumptions that allow us to ignore the boundary faces of T_I on ∂T. In particular, assume that B lies in the interior of T, so the sets b_I do not meet ∂T. If this is not the case, we may apply the argument below to level sets $b_I = \epsilon$, then take the limit as $\epsilon \to 0$. Since B is closed, we will obtain the desired result. Similarly, we will assume that the b_I's and the T_I's all intersect transversely.

We will use the transversality assumption that B does not meet ∂T in the arguments below. In particular, we will be considering the intersection of subsets of B with boundary faces of T_I. Since B does not meet ∂T, this allows us to ignore the faces of T_I which lie on ∂T in our argument.

Now, note the lemma will be immediately true if we can find some index j such that e_j is in the region T_j: for on e_j, $b_i = 0$ for all $i \neq j$, and in T_j, s_j is minimum. So assume this never happens.

Generally, if for some k-element set $I \subseteq \{1, \ldots, n\}$, $b_I \cap T_I$ is nonempty, we obtain a point which satisfies the lemma. So we will assume this also never happens. We will show that in this case, the point $(1, 1, \ldots, 1)$ is in B, thus concluding the proof. To prove this, we need another sublemma.

Lemma 4.5. *Let $\#(\cdot)$ denote the number of elements of a finite set. Assuming that each $b_I \cap T_I$ is empty,*

$$\sum_I \#(b_{I \cup \{n\}} \cap \partial T_I) \equiv \sum_J \#(b_{J \cup \{n\}} \cap \partial T_J) \equiv 1 \mod 2,$$

where the first sum is over all $(k+1)$-element subsets I of $\{1, \ldots, n-1\}$, and the second sum is over all k-element subsets J of $\{1, \ldots, n-1\}$.

Check that the statement of the lemma makes sense: Note if J is a k-element set, then $b_{J \cup \{n\}}$ is k-dimensional. T_J is $(n - k)$ dimensional, so its boundary faces are $(n-k-1)$-dimensional. Thus the intersections in the statement of the lemma are 0-dimensional manifolds, consisting of a finite number of points.

Also notice that when $k = (n-2)$ in the above lemma, there exists only one $(k+1)$-element subset I, namely $I = \{1, \ldots, n-1\}$. So $b_{I \cup \{n\}}$ is the whole set B. On the other hand, the boundary ∂T_I in this case must be the point in the intersection of all the T_i, or the point $(1, \ldots, 1)$. Thus the first sum counts the number of times the point $(1, \ldots, 1)$ appears in B. Hence, showing this number is odd will finish the proof of Lemma 4.4.

Proof. We prove Lemma 4.5 by induction on k.

We start by showing what essentially is the case $k = 0$. That is, we show

$$\sum_{i=1}^{n-1} \#(b_{\{i,n\}} \cap \partial T_i) \equiv \sum_{i=1}^{n-1} \#(e_n \cap T_i) \mod 2.$$

Since we are assuming $e_n \cap T_n = \emptyset$, the second sum in the above equation is just the number of points of e_n (since e_n is disjoint from each $T_i \cap T_j$ by transversality). That number of points is odd by Lemma 4.2, so this will give us the basis step of our induction.

Consider $b_{\{i,n\}} \cap T_i$. This is a 1–manifold, consisting of closed curves and arcs. Each arc has two endpoints. So

$$\sum_{i=1}^{n-1} \#\partial(b_{\{i,n\}} \cap T_i) \equiv 0 \mod 2.$$

On the other hand,

$$\sum_{i=1}^{n-1} \#\partial(b_{\{i,n\}} \cap T_i) = \sum_{i=1}^{n-1} \#(\partial b_{\{i,n\}} \cap T_i) + \sum_{i=1}^{n-1} \#(b_{\{i,n\}} \cap \partial T_i).$$

So $\sum_{i \neq n} \#(b_{\{i,n\}} \cap \partial T_i)$ has the same parity as $\sum_{i \neq n} \#(\partial b_{\{i,n\}} \cap T_i)$.

Consider $\partial b_{\{i,n\}} \cap T_i$. Note $\partial b_{\{i,n\}}$ consists of points in e_i and e_n. By assumption, e_i is never in T_i. Thus

$$\sum_{i=1}^{n-1} \#(\partial b_{\{i,n\}} \cap T_i) = \sum_{i=1}^{n-1} \#(e_n \cap T_i) = \#(e_n).$$

So $\sum_{i \neq n} \#(b_{\{i,n\}} \cap \partial T_i)$ is odd.

Our proof for general k follows essentially the same lines as the proof above.

Suppose $1 \leq k \leq n - 2$. We need to show

$$\sum_I \#(b_{I \cup \{n\}} \cap \partial T_I) \equiv \sum_J \#(b_{J \cup \{n\}} \cap \partial T_J) \mod 2,$$

where the first sum is over $(k+1)$-element subsets of $\{1, \ldots, n-1\}$ and the second is over k-element subsets.

Fix some $(k+1)$-element subset I, and again consider $b_{I \cup \{n\}} \cap T_I$. This is a 1–manifold. Its components are closed curves and arcs. Again

the number of endpoints of these arcs is even. So when we sum over all such I,

$$\sum_I \#\partial(b_{I\cup\{n\}} \cap T_I) \equiv 0 \mod 2.$$

On the other hand,

$$\sum_I \#\partial(b_{I\cup\{n\}} \cap T_I) = \sum_I \#(\partial b_{I\cup\{n\}} \cap T_I) + \sum_I \#(b_{I\cup\{n\}} \cap \partial T_I).$$

Thus we consider $\sum_I \#(\partial b_{I\cup\{n\}} \cap T_I)$. We want it to have the same parity as $\sum_J \#(b_{J\cup\{n\}} \cap \partial T_J)$, where J ranges over all k-element subsets of $\{1,\ldots,n-1\}$. We show now that the two sums are actually equal, which concludes the proof.

Consider $\partial b_{I\cup\{n\}}$. This consists of b_I, as well as things of the form $b_{I_j\cup\{n\}}$ where I_j is the k-element set obtained from I by removing the element $j \in I$. Since, by assumption, $b_I \cap T_I$ is empty, $\partial b_{I\cup\{n\}} \cap T_I$ is the union of sets $b_{I_j\cup\{n\}} \cap T_I$, where j ranges over all elements of I.

Then

$$(25)\qquad \sum_I \#(\partial b_{I\cup\{n\}} \cap T_I) = \sum_I \sum_{j\in I} \#(b_{I_j\cup\{n\}} \cap T_I).$$

We will change our method of counting in (25) above. Replace the terms I_j with k-element subsets J of $\{1,\ldots,n-1\}$. We will run through all such J. Then I will run through the $(k+1)$-element subsets given by $J \cup \{i\}$, where i is some element of $\{1,\ldots,n-1\} - J$. So the right hand side of equation (25) is equal to

$$\sum_J \sum_{i\in\{1,\ldots,n-1\}-J} \#(b_{J\cup\{n\}} \cap T_{J\cup\{i\}}).$$

On the other hand, we know the boundary ∂T_J is equal to the union of all faces $T_{J\cup\{j\}}$, where j ranges over all elements of $\{1,\ldots,n\} - J$. The only such face we are missing in our sum above is $T_{J\cup\{n\}}$. But by assumption, the intersection of $b_{J\cup\{n\}}$ with $T_{J\cup\{n\}}$ is trivial. Thus

$$\sum_J \sum_{i\in\{1,\ldots,n-1\}-J} \#(b_{J\cup\{n\}} \cap T_{J\cup\{i\}}) = \sum_J \#(b_{J\cup\{n\}} \cap \partial T_J).$$

<div align="right">q.e.d.</div>

This concludes the proof of Lemma 4.4. <div align="right">q.e.d.</div>

Lemmas 4.3 and 4.4 together give the desired bound on $\sum b_j$:

Theorem 4.6. *Let X be a hyperbolic manifold with $n + k$ cusps connected to a manifold M with k cusps by a cone deformation. (So in particular, there are n components of the singular locus, and cone angles at each component go from 0 to 2π.) Suppose during the deformation, the tube radius about the singular locus remains larger than $R_1 \geq 0.56$. Then*

the deformation can be parameterized so that at each time: $\min s_j = 1$ *and the sum of the boundary terms satisfies*

$$\sum_{j=1}^{n} b_j \leq n\, C(R_1).$$

Moreover, we can assume the deformation has reached the hyperbolic structure on M *by time* $t = (2\pi)^2$.

Proof. By Lemma 4.4, we may find a value S in T such that each $b_j(S) \geq 0$ and such that if for any index j, $s_j \neq \min\{s_1, \ldots, s_n\}$, then $b_j(S) = 0$. Denote the minimum value of the s_j by s: $s = \min\{s_1, \ldots, s_n\}$. Then Lemma 4.3 implies that

$$(26) \qquad \sum_{j=1}^{n} b_j = \sum_{\{j|b_j \neq 0\}} b_j \leq \sum_{\{j|b_j \neq 0\}} s^2\, C(R_1) \leq ns^2\, C(R_1).$$

First, we need to check that s is not equal to zero. Suppose not. That is, suppose $s = 0$. Then by (26), $\sum_{j=0}^{n} b_j = 0$. Recall that by equation (16) and the remark right after it, the sum of all b_j's equal zero only if the entire deformation is trivial. But this is possible only if each $s_j = 0$. Since the point $(0, 0, \ldots, 0)$ is not in the simplex T, this is impossible.

Now, recall the terms s_j affect the rate of change of the deformation. Thus we may rescale them without changing the tube radius. For the point S in T, divide each s_j by s. Replace S by this rescaled point, and denote the rescaled point by the same notation: $S = (s_1, \ldots, s_n)$. So each $s_j \geq 1$. Also, $s = \min\{s_j\} = 1$.

Thus equation (26) gives:

$$\sum_{j=1}^{n} b_j \leq n\, C(R_1).$$

Finally, to notice that the deformation is complete by time $t = (2\pi)^2$ as claimed, recall that if $s_j = 1$ throughout the deformation, then the cone angle is changing at a rate at which α_j will reach 2π at time $t = (2\pi)^2$. (See the discussion at the beginning of §4.1.) Since $s_j \geq 1$ always, the rate of change may only be faster. Thus each cone angle reaches 2π by the time $t = (2\pi)^2$. \hfill q.e.d.

When we combine Theorem 4.6 with the results of Theorem 3.3 and Theorem 3.6, we have completed the proofs of Theorems 1.2 and 1.3.

5. Bounding the meridian

We now show that the length of the shortest nontrivial simple closed curve on the cusp torus is bounded throughout the cone deformation, provided the tube radius about the singular locus stays large. Recall

here that we are calling this shortest curve the meridian of the torus. The following lemma is the last piece needed to complete the proof of Theorem 1.4.

Lemma 5.1. *Suppose M is a hyperbolic cone manifold with one cusp, and with singular locus Σ. Suppose the tube radius R about the singular locus is at least $\log(2/\sqrt{3})$. Then there exists a horoball neighborhood U of the cusp such that the meridian of ∂U has length at least $1 - e^{-2R}$.*

Proof. Let $X = M - \Sigma$. X admits an incomplete hyperbolic metric. Expand the tube $V = \cup V_i$ about the singular locus Σ until the tube hits itself. Each V_i has the same tube radius R. Next expand the horoball U about the cusp until it either becomes tangent to itself or to V.

We obtain a region Ω by continuing to expand U as follows. First, choose a particular lift U_a of U in the universal cover. Because U is embedded in $\mathbb{H}^3$ by the developing map on the universal cover $\widetilde{X}$ of X, we can assume the developing map is one to one on U_a and takes ∂U_a to the plane $z = 1$ in $\mathbb{H}^3$.

Take $\Omega = U_a \cup S$, where S is the set consisting of all points x in $\widetilde{X}$ such that the distance $\text{dist}(x, \partial U_a) < \text{dist}(x, \partial U_b)$ for U_b any other lift of U, and also such that the distance $\text{dist}(\phi(x), \partial U) < \text{dist}(\partial U, \Sigma)$, where ϕ is the covering projection. Note that Ω is embedded in $\mathbb{H}^3$ by the developing map. That is, the developing map is one to one on Ω.

Let p be a point on ∂U closest to Σ, and let p_0 and p_1 be lifts of p on ∂U_a such that the projection of the path from p_0 to p_1 is shortest on ∂U. Let a_0 be the point in the universal cover on a lift of Σ such that the path from p_0 to a_0 has length equal to the minimum distance from p_0 to Σ. Similarly, let a_1 be the point on a lift of Σ such that the path from p_1 to a_1 has length equal to the minimum distance from p_1 to Σ. Note the interiors of the paths between p_0 and a_0 and between p_1 and a_1 are contained in Ω.
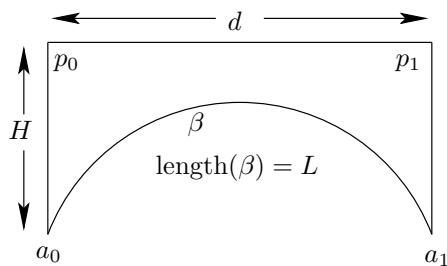

Figure 3. The top edge of the quadrilateral maps to the shortest path on ∂U under the covering projection.

Then note that the interior of the geodesic β from a_0 to a_1 is also in Ω, along with all the points in the quadrilateral with sides given by β

and the paths from p_0 to p_1, from p_0 to a_0, and from p_1 to a_1. This is because, first, all points x in this quadrilateral (except the endpoints of β) have $\mathrm{dist}(\phi(x), \partial U) < \mathrm{dist}(\partial U, \Sigma)$. Also, if any x were closer to some other lift U_b of U, then there would be points in the quadrilateral equidistant to two different lifts of U. All points equidistant to two different lifts of U lie on some totally geodesic planes of $\mathbb{H}^3$. Hence some geodesic must intersect β but not the paths from p_0 to a_0, p_1 to a_1, or the path on the horosphere ∂U_a from p_0 to p_1. This is impossible.

Now let H be the length of the paths from p_0 to a_0 and from p_1 to a_1. Let L be the length of β. We know that $H \geq R$ and $L \geq 2R$ since the distance between any two components of the lift of Σ is greater than or equal to $2R$. We let d be the length of the path on the horosphere ∂U_a between p_0 and p_1. Since Ω is embedded by the developing map, we can assume the quadrilateral is of the form shown in Figure 3.

Then solving for d in terms of H and L, $d = 2e^{-H}\sinh(L/2)$.

Case 1: $H = R$. Then $d \geq 2e^{-R}\sinh(R) = 1 - e^{-2R}$.

Case 2: $H > R$. Then U must be tangent to itself, say at a point q, and not necessarily tangent to the tube about Σ. Then the image of Ω under the developing map must contain some portion of the region above the geodesic surface equidistant from a horizontal plane (the lift of ∂U_a) and some other horosphere.

This geodesic surface is some portion of the (Euclidean) hemisphere with radius 1, tangent to the lift of ∂U_a at a lift q_0 of q. See Figure 4. The image of Ω under the developing map contains a neighborhood of points on this hemisphere about q_0. If it were to contain all the points on the hemisphere between the dotted lines in Figure 4 (that is, points whose projection to $\mathbb{C}$ have Euclidean distance at most $1/2$ from the projection of q_0 to $\mathbb{C}$), then $d \geq 1$.

Let x be one of these points. That is, the projection of x to $\mathbb{C}$ has Euclidean distance at most $1/2$ from the projection of q_0 to $\mathbb{C}$. Note x will lie in Ω provided $\mathrm{dist}(\phi(x), \partial U) < \mathrm{dist}(\partial U, \Sigma) = H$, or provided H is large enough. But now, $\mathrm{dist}(\phi(x), \partial U) = \log(1/\mathrm{height}(x))$, where $\mathrm{height}(x)$ denotes the z–coordinate of x in $\mathbb{H}^3$. Thus this distance is at most $\log(2/\sqrt{3})$.
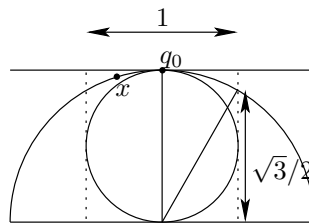

Figure 4.

Since $H > R$, we can ensure $d \geq 1$ by restricting to $R \geq \log(2/\sqrt{3})$.
q.e.d.

When we plug the result of Lemma 5.1 into Theorem 3.8, along with the bound on $\sum b_j$ of the previous section, we may complete the proof of Theorem 1.4.

Theorem 1.4.   *Let $M = X_\tau$ be a hyperbolic 3–manifold with a cusp, and let $X = X_0$ be a hyperbolic 3–manifold which can be joined to M by a smooth family of hyperbolic cone manifolds X_t with tube radius at least $R_1 \geq 0.56$, and with n components of the singular locus. Let U_t be a horoball neighborhood about the cusp. Let $h(M)$ denote the normalized height of the cusp torus ∂U_τ. Let $h(X)$ denote the normalized height of ∂U_0. Then the hyperbolic cone deformation can be parameterized such that the change in normalized height is bounded in terms of R_1 alone:*

$$-(2\pi)^2 \frac{\sqrt{n\,C(R_1)}}{(1 - e^{-2R_1})\sqrt{2}} \leq h(M) - h(X) \leq (2\pi)^2 \frac{\sqrt{n\,C(R_1)}}{(1 - e^{-2R_1})\sqrt{2}}.$$

Proof. Theorem 3.8, combined with Theorem 4.6 and Lemma 5.1, implies that

$$-\frac{\sqrt{n\,C(R_1)}}{(1 - e^{-2R_1})\sqrt{2}} \leq \dot{h} \leq \frac{\sqrt{n\,C(R_1)}}{(1 - e^{-2R_1})\sqrt{2}}$$

and that the total time of the deformation is $t = (2\pi)^2$. We integrate the above inequality over the deformation. The bounds on the left and right are independent of t. Thus we obtain the conclusion of the theorem. q.e.d.

6. Cusp shapes of hyperbolic knots

We will now apply the results of the previous sections to determine bounds on the shapes of cusps of knot complements. In particular, let K be a hyperbolic knot with a prime, twist reduced diagram, where prime and twist reduced are defined in Definitions 1.6 and 1.7. We will bound the normalized height of the cusp of $S^3 - K$, using Theorem 1.4. We need the following:

1) An initial hyperbolic manifold X with $n + 1$ cusps.
2) A cone deformation deforming X to the knot complement $S^3 - K$.
3) A lower bound on the tube radius ($R \geq R_1 \geq 0.56$).

Given these pieces, we will obtain bounds on normalized height.

6.1. An initial manifold. Begin with a prime, twist reduced diagram of the knot K. At each twist region of the diagram, add a closed curve encircling two strands, called a *crossing circle*. We now have a diagram of a link, which we call J. The link complement $S^3 - J$ is homeomorphic

to the complement of the link L obtained from J by removing pairs of crossings from each twist region. See Figure 5.
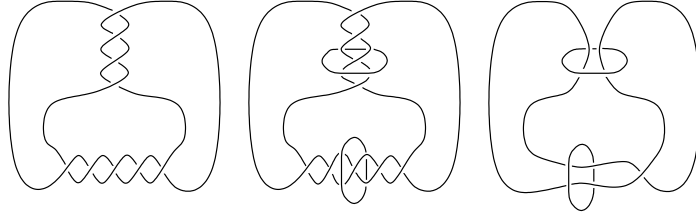

Figure 5. Left to right: The link K. The link K with crossing circles added. The link L.

These links with crossing circles added have been studied by many people, including Adams [**1**], Lackenby, Agol and Thurston [**16**]. Many of the properties of these links were addressed in previous papers (see [**21**], and [**12**] with Futer).

The links are useful to us in the cone manifold setting because first of all, symmetries of the diagram of L allow us to determine the hyperbolic structure on $S^3 - L$ explicitly. Secondly, $S^3 - L$ is related to the original knot complement via Dehn filling. In particular, if $2m_i$ crossings were removed from the i-th twist region to go from the diagram of J to that of L, then by performing a $1/m_i$ Dehn filling on the corresponding i-th crossing circle of $S^3 - L$, we re-insert these crossings and put back the crossing circle, obtaining $S^3 - K$ (see e.g., [**22**], Chapter 9).

Thus, starting with a hyperbolic augmented link L, we can determine information including shapes of the cusps. Next, we can find conditions which will ensure the Dehn filling above can be obtained by a hyperbolic Dehn filling via cone deformation. Hence we will have the first two pieces needed to bound the normalized height of the cusp K: The initial manifold M with hyperbolic structure will be $S^3 - L$. It will be connected by cone deformation to $S^3 - K$.

6.1.1. The geometry of $S^3 - L$. We note in [**12**] that if K has at least 2 twist regions, then the augmented link complement $S^3 - L$ will admit a complete, finite volume hyperbolic structure. This can be shown by work of Adams [**1**], using the geometrization of Haken manifolds. It can also be shown more directly using Andreev's theorem. The proof using Andreev's theorem gives a packing of circles related to $S^3 - L$ which we will need again in Section 6.4, so we include it here.

Theorem 6.1. *If K has a prime, twist reduced diagram with at least 2 twist regions, then the augmented link complement $S^3 - L$ will admit a complete, finite volume hyperbolic structure.*

Proof. We prove the lemma by finding the hyperbolic structure. To do so, we decompose $S^3 - L$ into two ideal polyhedra, as in [**16**] and

[**12**]. We then find a hyperbolic structure on the polyhedra which gives a nonsingular hyperbolic structure on $S^3 - L$ after gluing.

To find the polyhedra, first remove all remaining single crossings at crossing circles. That is, if the number of crossings in a twist region of the diagram of K was odd, then $S^3 - L$ will still have a single crossing at that twist region. Remove it. The new link has components lying flat in the projection plane bound together by crossing circles. Call it L'.

Slice $S^3 - L'$ along the projection plane. This cuts the manifold into two identical pieces, one on either side of the plane. Each 2–punctured disk encircled by a crossing circle has been sliced in half. Slice along these remaining halves of disks, opening them up into two faces. This gives an ideal polyhedral decomposition of the manifold. The edges are given by the intersection of the 2–punctured disks with the projection plane. On each of the two polyhedra, we have one face per planar region of the diagram of L', and two triangular faces per 2–punctured disk. Shade the faces arising from 2–punctured disks, giving each polyhedron a checkerboard coloring. The edges meet in 4–valent ideal vertices. At each vertex, two white faces are separated by two shaded faces. (See [**12**] or [**16**] for pictures.)

The gluing pattern on the polyhedra is given by following the above process in reverse: First, on each polyhedron fold the pairs of triangular shaded faces together at their common vertex. Then glue each white face to its corresponding face on the opposite polyhedron via the identity map. This gives back $S^3 - L'$.

To obtain $S^3 - L$, we use the same two polyhedra, but make the following change in gluing. For crossing circles encircling a single crossing of the diagram of L, rather than glue shaded triangles across their common vertex on a single polyhedron, we insert a half–twist by gluing each triangle of one polyhedron to the opposite triangle of the other. See Figure 6.
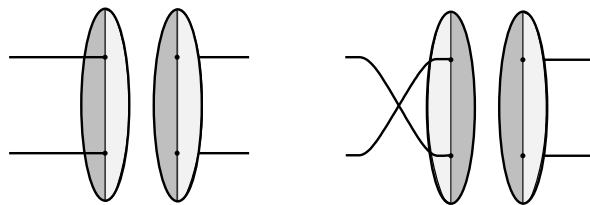

Figure 6. Left: Gluing 2–punctured discs with no crossings. Right: Gluing 2–punctured discs with a single crossing.

Now our goal is to find a hyperbolic structure on these two polyhedra. We show the two polyhedra actually have totally geodesic faces in $\mathbb{H}^3$,

meeting in dihedral angles of $\pi/2$. Since faces are glued in pairs, and edges in 4's, the gluing will give a complete hyperbolic structure on $S^3 - L$.

Note any totally geodesic plane in $\mathbb{H}^3$ extends to give a circle on the boundary S^2 at infinity. Conversely, given a collection of circles on S^2, we can view those circles as boundaries of planes in $\mathbb{H}^3$. We obtain our polyhedra by finding appropriate circle packings, then cutting away half–spaces bounded by hemispheres in $\mathbb{H}^3$. Our tool is a corollary of Andreev's theorem noted by Thurston in [**23**]:

Theorem 6.2 (Andreev). *Let γ be a triangulation of S^2 such that each edge has distinct ends and no two vertices are joined by more than one edge. Then there is a packing of circles in S^2 whose nerve is isotopic to γ. This circle packing is unique up to Möbius transformation.*

Recall that the *nerve* of a circle packing is the graph obtained by adding a vertex for each circle, and an edge connecting two vertices if and only if the corresponding circles are tangent.

We begin by finding a triangulation of S^2 associated with one of the polyhedra described above. For each white face, take a vertex. Connect two vertices by an edge if and only if the two corresponding white faces meet at a vertex of the polyhedron. This gives a triangulation γ of S^2. Note if we draw vertices of γ on top of white faces of the polyhedron, and edges of γ through the vertices of the polyhedron, that each triangle of γ circumscribes a shaded face of the polyhedron.

To apply Andreev's theorem, we need to show this triangulation γ satisfies the conditions: each edge has distinct ends, and no two vertices are joined by more than one edge. To show these conditions, we consider the graph dual to γ, as follows.

Consider the original link diagram. We view it as a 4–valent graph. Replace each twist region of the graph by a single edge, as in Figure 7.
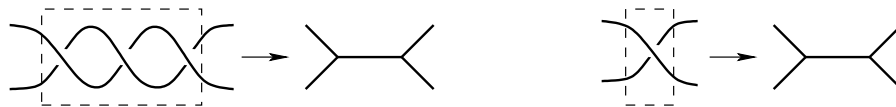

Figure 7. Create a trivalent graph by replacing each twist region with an edge.

Since each crossing is part of some twist region, this gives a trivalent graph Γ. Note the dual graph to Γ is isotopic to the triangulation γ. We use properties of the dual Γ to show the triangulation γ satisfies the conditions necessary for Andreev's theorem.

Lemma 6.3. *No edge of γ has a single vertex at both endpoints.*

Proof. Consider the graph Γ. If its dual γ has an edge with one vertex at both endpoints, then the graph Γ must be of the form in Figure 8 (a).
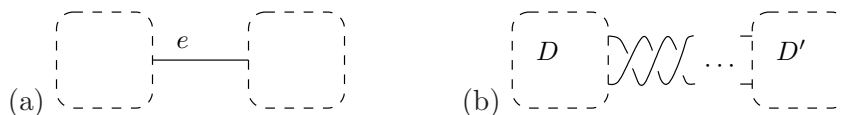

Figure 8. (a.) Form of Γ if γ has an edge with a single vertex at both endpoints. (b.) Corresponding form of original link diagram.

Note then if the edge e was an original edge of the 4–valent link diagram, then we have a simple closed curve intersecting the link diagram transversely in a single point. This is impossible.

If instead the edge e replaced a twist region in the original 4-valent link diagram, then the original diagram had the form of Figure 8 (b). However, note that one of the subdiagrams D and D' must contain crossings else the original diagram has at most one twist region. Without loss of generality, say D contains crossings. Then the dashed simple closed curve enclosing D intersects the link diagram transversely in two points, but both its interior and its exterior contain crossings. This contradicts the fact that the original diagram was prime.   q.e.d.

Lemma 6.4. *No two vertices of γ are joined by more than one edge.*

Proof. Suppose two vertices of γ are joined by two distinct edges. Then consider the dual graph Γ. Γ must be of the form shown in Figure 9 (a), where region B and region B' are the same.

Give the edge e_1 an orientation, say e_1 points in the direction of the edge a. This gives the region A an orientation, and hence assigns to the edge e_2 an orientation. Now, trace a path of edges around the region B, listing the edges in the order they occur. Our list begins with e_1, then a, etc. Note e_2 must appear in the list before the edge d, else region B would be cut off from region B'. Also, edge b must occur before edge c, by the orientation on e_2. Hence the graph Γ has the form illustrated in Figure 9 (b).

Case 1: Edges e_1 and e_2 both were edges of the original 4–valent link diagram. Then there is a simple closed curve intersecting e_1 and e_2 transversely in the original link diagram and intersecting the diagram in no other points. Since the original diagram has crossings on either side of the region A, this contradicts the fact that we started with a prime diagram.
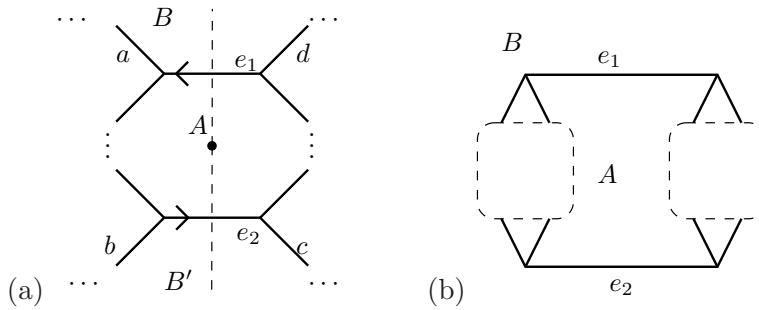
Figure 9. Form of Γ when γ has two vertices connected by two distinct edges. In (a), the edges of γ are the dashed lines, with one of the vertices in A and the other at ∞.

Case 2: Edges e_1 and e_2 both replaced twist regions in the original link diagram. Then the original link diagram must have been of the form in Figure 10 (a). Then since the original diagram was twist reduced, either the subdiagram D or D' must be a string of bigons. But then rather than two distinct twist regions, our diagram must have had only one twist region. Thus edges e_1 and e_2 would not have been distinct.
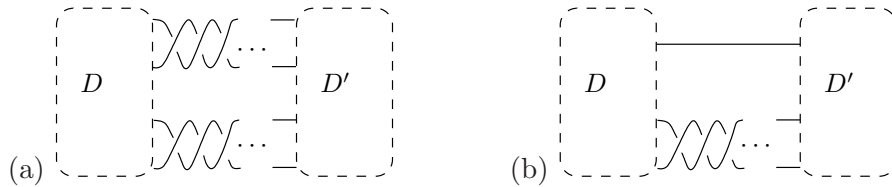
Figure 10. Possible forms of the original link diagram if γ contains two vertices connected by two distinct edges.

Case 3: One of edge e_1 or e_2 is from the original link diagram, the other replaced a twist region. Then the original link diagram must have been of the form shown in Figure 10 (b). Now note that the simple closed curve bounding subdiagram D intersects the link transversely in only three points. This is impossible.

Since these are the only three cases, these contradictions prove the lemma.   q.e.d.

Now Lemmas 6.3 and 6.4 are enough to show that Andreev's theorem applies, and there is a circle packing of S^2 whose nerve is γ.

Complete the proof of Theorem 6.1 by slicing off half–spaces bounded by geodesic hemispheres in $\mathbb{H}^3$ corresponding to each circle in the circle packing. These give the geodesic white faces of the polyhedron. The

shaded faces are obtained by slicing off hemispheres in $\mathbb{H}^3$ corresponding to each circle of the dual circle packing. Note white and shaded hemispheres meet at right angles.

Thus the polyhedron for the flat augmented link is totally geodesic in $\mathbb{H}^3$, and hence the flat augmented link is hyperbolic.   q.e.d.

6.1.2. Normalized lengths on cusps. To apply results on cone deformations, we will need the following information on normalized lengths of particular curves on the cusps of $S^3 - L$.

Proposition 6.5. *Let K and L be as above. In the prime, twist reduced diagram of K, let n be the number of twist regions. Let c_i be the number of crossings in the i-th twist region. Then on cusps of L, we have the following normalized lengths.*

1) *For a cusp corresponding to a crossing circle, let s_i be the slope such that Dehn filling $S^3 - L$ along s_i re-inserts the c_i crossings at that twist region. Then the normalized length of s_i is at least $\sqrt{c_i}$.*
2) *For the cusp corresponding to the link component in the projection plane, the normalized height (i.e., the normalized length of the curve orthogonal to a meridian) is at least $\sqrt{n}$, and at most $\sqrt{n(n-1)}$.*

Proof. This can be deduced from results of [**12**]. However, given the circle packing associated to $S^3 - L$ developed in the previous section, we are able to streamline the proof somewhat.

First, recall the polyhedra obtained in the proof of Theorem 6.1. Note each cusp will be tiled by rectangles given by the intersection of the cusp with the totally geodesic white and shaded faces of the polyhedra. Two opposite sides of each of these rectangles come from the intersection of the cusp with shaded faces of the polyhedra, or from the 2–punctured disks in the diagram of L, and the other two sides come from white faces. Call the sides shaded sides and white sides, respectively.

For part (1), note any crossing circle intersects a single 2–punctured disk in a longitude. Half of the longitude is given by the intersection with one polyhedron, the other half by intersection with the other. The crossing circle intersects no other shaded faces. Thus the crossing circle cusp is tiled by exactly two identical rectangles.

When the crossing circle encircles no single crossing, or half twist, then two white faces intersect the cusp in meridians. In this case, c_i is even, $c_i = 2m_i$, and the slope s_i is $1/m_i$. It is given by one step along a white side of a rectangle (a meridian), plus $2m_i = c_i$ steps along shaded sides of the rectangle.

When the crossing circle encircles a single crossing, then the two rectangles tiling the cusp are sheared. In this case, a meridian is given by one step along a white side, plus (or minus) a step along a shaded

side. Now $c_i = 2m_i + 1$ is odd, and the slope $s_i = 1/m_i$ is given by a step along a white side, plus (or minus) a step along a shaded side, plus (or minus) $2m_i$ steps along shaded sides.

In either case, the slope is given by a single step along a white side plus (or minus) c_i steps along a shaded side. Let w denote the length of a white side, and let s denote the length of a shaded side. Thus the normalized length of s_i is:

$$\frac{\sqrt{w^2 + c_i^2 s^2}}{\sqrt{2ws}} = \sqrt{\frac{w}{2s} + c_i^2 \frac{s}{2w}}.$$

Let $u = w/(2s)$. Then for constant c_i, this quantity is minimized when $u = c_i/2$, and the minimum value is $\sqrt{c_i}$.

For part (2), we need to know more about the possible lengths of the white sides of rectangles tiling the cusp. For a given rectangle, consider the corresponding vertex in one of the polyhedra. On the sphere S^2 at infinity, this vertex will look like a point of tangency of two circles in the packing given by Andreev's theorem. Since the nerve of this circle packing is a triangulation of S^2, the point of tangency corresponds to an edge on two distinct triangles of this nerve. Thus there are two additional circles tangent to the two given circles, as in Figure 11.
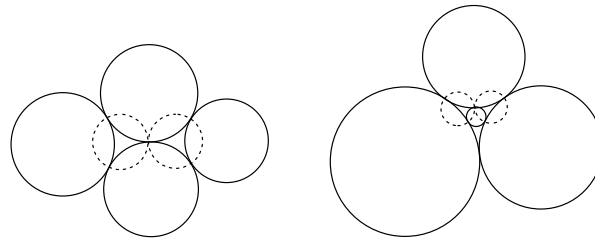

Figure 11. The form of the packing of circles about any vertex. Dashed circles correspond to the shaded faces of the polyhedron at this vertex.

Now, apply a Möbius transformation taking the vertex, or the point of tangency of the circle packing, to infinity. This takes the two tangent circles to two parallel lines. It takes the two additional tangent circles to circles tangent to both the parallel lines, as in Figure 12. Note this also gives the similarity structure of the rectangle under consideration. If we normalize so that the shaded side (coming from the intersection with a 2–punctured disk) has length 1, then the circle lying under the dashed line in Figure 12 has diameter 1. Since circles in the circle packing do not overlap, this forces a white side (i.e., without dashes in the figure) to have length at least 1.
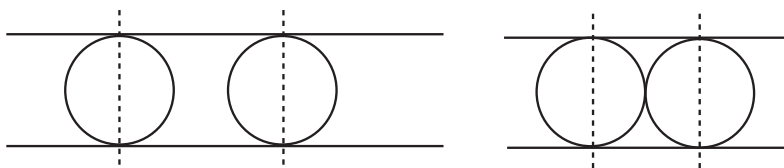
Figure 12. Result of taking point of tangency to infinity.

For an upper bound on the length of a white side, note it is longest when all circles in the circle packing are lined up in a row, tangent to the two parallel lines. In this case, when a shaded side has length 1, the length of the white side will be the number of circles between the parallel lines, minus 1. To find the number of circles possible, we use an Euler characteristic argument. Note there will be $2n$ shaded faces in one of the polyhedra, coming from opening up n crossing circles. These each correspond to a single face of the triangulation of S^2 used in Andreev's theorem. Because it is a triangulation, the number of edges equals $3/2$ the number of faces, or $3n$. Then by an Euler characteristic argument, there are $n + 2$ vertices. Recall each vertex gave a circle in our circle packing. Since two of these circles become our parallel lines, there are n circles packed between these. Thus the maximum length of a white side is $n - 1$.

Now, note that the cusp in the projection plane intersects each 2–punctured disk $2n$ times, each time in a meridian. Half of this meridian will come from the intersection of one polyhedron (the "top" half), the other half from the intersection of the other polyhedron. Thus the meridian runs along two shaded sides of rectangles. Still normalizing so each shaded side has length 1, this implies a meridian has length 2. The curve giving the height H of the cusp runs along $2n$ white sides of the rectangles (one for each 2–punctured disk of intersection). The normalized height will be given by $H/\sqrt{2H} = \sqrt{H/2}$. The height H will be minimal when each of the $2n$ white sides it runs along are of minimal length, or length 1. Thus the minimal normalized height is $\sqrt{n}$.

Similarly, the height H will be maximal when each white side is of maximal length, or length $n - 1$. Thus the maximal normalized height is $\sqrt{n(n-1)}$.   q.e.d.

6.1.3. Hyperbolic cone deformation on $S^3 - L$. If the normalized lengths of the slopes on which Dehn filling was performed were sufficiently large, then Hodgson and Kerckhoff showed that the Dehn filling could be realized by a hyperbolic cone deformation [**14**]. Proposition 6.5 indicates that to attain these minimal normalized slope lengths, we need only ensure that there are sufficiently many crossings in each twist region. In particular, by [**14**], provided $\sqrt{c_j} \geq 10.6273$, or provided

that there are at least 113 crossings per twist region of the prime, twist reduced diagram of K, then the Dehn filling of $S^3 - L$ can be realized by a hyperbolic cone deformation.

Actually, we will see that the number of crossings in each twist region needs to be larger than 113 to apply Theorem 4.6. For now, however, note that we may ensure a hyperbolic cone deformation does exist from $S^3 - L$ to $S^3 - K$ by putting conditions on the diagram of K.

6.2. Finding values for tube radius. We need to ensure that the tube radius remains larger than $R_1 = 0.56$ throughout the cone deformation. We can do so by again applying work of Hodgson and Kerckhoff [**14**]. They show that in the neighborhood of the j-th component of the singular locus, we can increase the cone angle from 0 to 2π, maintaining the tube radius $R \geq R_1$, provided equation (24) of the proof of Lemma 4.3 holds.

That is, consider a particular component of the singular locus Σ_j. The singular locus consists of crossing circles of the link L. At the j-th crossing circle, the hyperbolic cone deformation performs Dehn filling along a slope of the form $1/n_j$. Let L_0 denote the normalized length of this slope in $S^3 - L$. We can then increase the cone angle from 0 to 2π, maintaining the tube radius bound $R \geq R_1$, provided the normalized length L_0^2 is larger than the increasing function $I(R_1)$ defined in equation (24).

So to ensure $R \geq R_1 \geq 0.56$, we compute that L_0^2 must be at least 113.044. By Proposition 6.5, we know L_0^2 is at least c_i, where c_i is the number of crossings in the i-th twist region. Thus by ensuring there are at least 114 crossings in the i-th twist region, we will guarantee that our tube radius is at least 0.56. For general R_1, we have the following result.

Lemma 6.6. *Let K, L be as above, such that we have a cone deformation from $S^3 - L$ to $S^3 - K$. Fix $R_1 \geq 0.531$. Then $R \geq R_1$ throughout the deformation provided the number of crossings in each twist region is at least $I(R_1)$, where $I(R_1)$ is defined in equation (24).*

6.3. Proof of Theorem 1.8.

Theorem 1.8. *Let K be a knot in S^3 which admits a prime, twist reduced diagram with a total of $n \geq 2$ twist regions, with each twist region containing at least $c \geq 116$ crossings. In a hyperbolic structure on $S^3 - K$, take a horoball neighborhood U about K. Normalize so that the meridian on ∂U has length 1. Then the height H of the cusp of $S^3 - K$ satisfies:*

$$H \geq n \left(1 - f(c)\right)^2.$$

Here $f(c)$ is a positive function of c which approaches 0 as c increases to infinity. Additionally, $H \leq n(\sqrt{n-1} + f(c))^2$.

Proof. If K admits a prime, twist reduced diagram with at least 2 twist regions, then we may form the augmented link L from the diagram of K. We have seen in §6.1.3 that, provided there are at least 113 crossings in each twist region of the diagram of K, then $S^3 - L$ and $S^3 - K$ are connected by a hyperbolic cone deformation X_t, with $X_0 = S^3 - L$, $X_\tau = S^3 - K$. The singular locus will consist of the crossing circle components of L. There will be n of these.

By results of Section 6.2, if there are at least 114 crossings per twist region then the tube radius of the deformation is at least $R_1 = 0.56$. Then by Theorem 1.4,

$$-(2\pi)^2 \frac{\sqrt{n\,C(R_1)}}{(1 - e^{-2R_1})\sqrt{2}} \leq h_\tau - h_0 \leq (2\pi)^2 \frac{\sqrt{n\,C(R_1)}}{(1 - e^{-2R_1})\sqrt{2}},$$

where h_t denotes the normalized height of the cusp at time t.

And so:

$$(27) \qquad h_0 - (2\pi)^2 \frac{\sqrt{n\,C(R_1)}}{(1 - e^{-2R_1})\sqrt{2}} \leq h_\tau \leq h_0 + (2\pi)^2 \frac{\sqrt{n\,C(R_1)}}{(1 - e^{-2R_1})\sqrt{2}}.$$

We may now apply part (2) of Proposition 6.5. This implies that the initial normalized height h_0, i.e., the normalized height on $S^3 - L$, is between $\sqrt{n}$ and $\sqrt{n(n-1)}$.

Plug this into the left hand side of the above equation and we find:

$$(28) \qquad h_\tau \geq \sqrt{n}\left(1 - (2\pi)^2 \frac{\sqrt{C(R_1)}}{(1 - e^{-2R_1})\sqrt{2}}\right).$$

For the right hand side, we find:

$$(29) \qquad h_\tau \leq \sqrt{n}\left(\sqrt{n-1} + (2\pi)^2 \frac{\sqrt{C(R_1)}}{(1 - e^{-2R_1})\sqrt{2}}\right).$$

The term $C(R_1)$ can be computed explicitly using the formulas in the proof of Lemma 4.3. Recall $C(R_1)$ is strictly decreasing, approaching 0 as R_1 approaches infinity. Thus the function

$$\bar{f}(R_1) = (2\pi)^2 \frac{\sqrt{C(R_1)}}{(1 - e^{-2R_1})\sqrt{2}},$$

which appears in both (28) and (29), is decreasing with R_1, approaching 0. The graph of $\bar{f}$, as well as that of $I(R)$, is shown in Figure 13.

When $R_1 = 0.56$, $1 - \bar{f}(R_1)$ is negative. Since h_τ is known to be positive, this doesn't give a very good estimate in (28). To get a better estimate, we increase R_1. The value $1 - \bar{f}(R_1)$ becomes positive when R_1 is about 0.6624. However, as R_1 increases, so does $I(R_1)$, so by Lemma 6.6, we need to increase the number of crossings in each twist region to guarantee that the tube radius remains larger than R_1 throughout the deformation. In particular, c must be at least 116 to ensure $R_1 \geq 0.6624$.
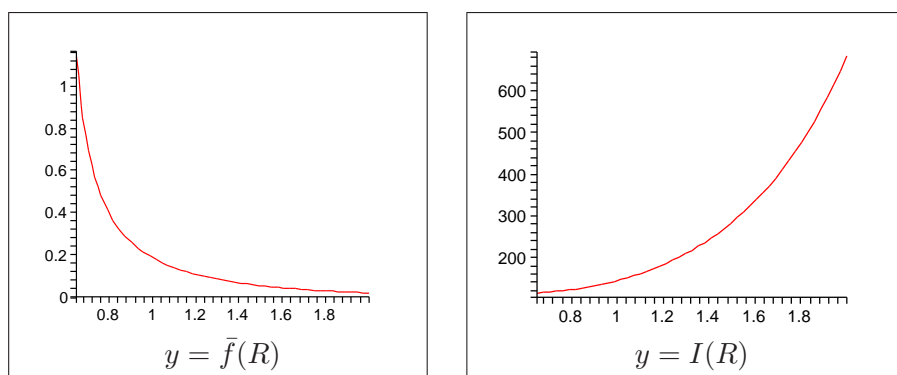
Figure 13. Graphs of $\bar{f}(R)$ and $I(R)$. Here $\bar{f}(R)$ gives the bounds in Theorem 1.8 for given tube radius R. $I(R)$ gives the number of crossings required to guarantee tube radius R.

In general, let $f(c) = \bar{f}(I^{-1}(c))$. Since $I(R)$ is strictly increasing for $R \geq 0.56$, this is well defined. Then for $c \geq 116$, $1 - f(c)$ is positive.

To finish the proof, note that we can scale so that the meridian of the cusp of $S^3 - K$ has length 1. Then the actual height H of the cusp of $S^3 - K$ will be at least $(h_\tau)^2$. q.e.d.

Notice in Figure 13 that $\bar{f}$ is close to 0 for values of R near 2. However, for R this size, $I(R)$, or the number of crossings required per twist region, is nearly 700. We find a nice compromise by choosing $R = 1.0$. Then $I(R)$ is not much larger than 116, and yet $1 - \bar{f}$ is already over 0.8. We use this fact in the following corollary, which gives more explicit numbers to the results of Theorem 1.8.

Corollary 6.7. *Let K be as in the previous theorem, with at least $c \geq 145$ crossings in each twist region. Then when the meridian of the cusp of $S^3 - K$ is normalized to have length 1, the height of the cusp satisfies:*

$$H \geq n \, (0.81544)^2.$$

Proof. Letting $c \geq 145$ in the above theorem ensures that $R > R_1 = 1.0$. Then $1 - f(c) = 1 - \bar{f}(1.0) \geq 0.81544$. q.e.d.

6.4. Example: 2–bridge knots. The requirement of Theorem 1.8 that there be at least 116 crossings per twist region was based on the worst case analysis. This came from Proposition 6.5, in which we showed that in the worst possible case, the normalized length of a slope was at least the square root of the number of crossings. When we are dealing

with particular classes of knots, we can often make significantly better estimates, and reduce the number of crossings required. In this section, we present a particular example of such a class of knots: 2–bridge knots.

We will determine the circle packing obtained from the proof of Theorem 6.1 for a 2–bridge knot. A 2–bridge knot with an even number of twist regions will have a corresponding augmented link L of the form of Figure 14, except possibly with single crossings added at some crossing circles. The picture for an odd number of twist regions is similar.
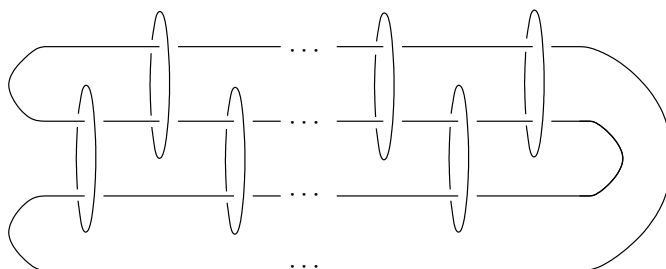

Figure 14. Augmented link of a 2–bridge knot with an even number of twist regions, and an even number of crossings per region.

In any case, the link will correspond to a trivalent graph Γ of the form shown in Figure 15. Note each region of the graph complement gives a circle in the circle packing, with tangencies across edges. Thus each circle will be tangent to the circles corresponding to regions A and D. The circle packing associated with this graph is of the form in Figure 16.
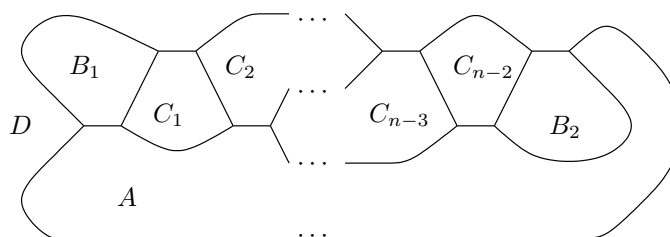

Figure 15. Trivalent graph associated with a 2–bridge knot.

Recall that the shape of cusps can be determined by analyzing the rectangles we get from taking points of tangency of the circles in Figure 16 to infinity. In particular, we are interested in the cusp shapes which correspond to crossing circles in the link L. The rectangles tiling these cusps come from the tangencies of circle A with certain of the B_i and
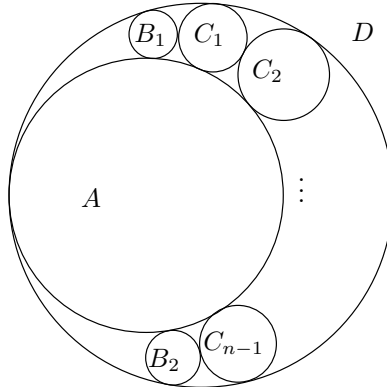
Figure 16. Circle packing associated with a 2–bridge knot.

C_i, and from tangencies of D with certain of the B_i and C_i. Thus we find the general shape of rectangles of this form.

When we take a point of tangency between A and B_i to infinity, $i = 1$ or 2, the two circles tangent to both A and B_i are D and a C_j. These are tangent to each other. Thus our rectangle in this case is a square. Similarly for points of tangency between D and B_i.

A crossing circle coming from one of these points of tangency will therefore be tiled by two squares, with a longitude running across two shaded sides. Then the slope s_i along which Dehn filling is performed will have normalized length $\sqrt{1 + c_i^2}/\sqrt{2}$. Note this is larger than $I(0.6624)$, implying that the results of Theorem 1.8 apply, provided $c_i \geq 16$. It is larger than $I(1.0)$, implying the results of Corollary 6.7 hold, when $c_i \geq 17$. Thus the number of crossings in our theorem has gone from 116 to 16, and 145 to 17.

When we take a point of tangency between A and C_i, or between D and C_i to infinity, we get a 1 by 2 rectangle. This is because the circles A and C_i are tangent to two distinct circles C_{i-1} and C_{i+1}, or possibly a B_i, which are each tangent to D. Since D is also tangent to A and C_i, in the picture at infinity we have two parallel lines, A and C_i, with three full sized circles tangent to each other and also to the lines A and C_i.

In this case, the crossing circle is tiled by two 1 by 2 rectangles, stacked to form a square. The slope s_i will have normalized length $\sqrt{4 + c_i^2}/\sqrt{4}$. It will be larger than $I(0.6624)$ provided $c_i \geq 22$, and larger than $I(1.0)$ provided $c_i \geq 24$.

We can also make improvements on the initial normalized height, i.e., the value $h(X)$ of Theorem 1.4. To compute $h(X)$, we determine the shape of the rectangles tiling the cusp corresponding to the knot strand.

These include all rectangles obtained by taking a point of tangency of the circle packing of Figure 16 to infinity, except those tangencies corresponding to crossing circle cusps.

Each circle tangency of the form C_{2k} tangent to D will give a rectangle on the knot strand cusp. Similarly, those tangencies of circles C_{2k+1} tangent to A will give rectangles on the knot strand cusp. As we saw above, these rectangles will each have dimensions 1 by 2. The side of length 2 will contribute to the height. There will be $(n-2)$ of these rectangles, since each C_j contributes one. Thus these rectangles contribute $2n-4$ to the height.

Each circle tangency C_i tangent to C_{i+1} also gives a rectangle on the knot strand cusp, as do the tangencies B_1 with C_1 and C_{n-2} with B_2. Each of these rectangles is a square, contributing 1 to the height, and there are $(n-1)$ such rectangles.

The tangencies of B_1 and D and of B_2 and A (or D if n is odd) also contribute rectangles of dimension 1 by 1 to the knot strand. Finally, the tangency of A to D gives a rectangle with dimensions 1 by $(n-1)$, contributing $(n-1)$ to the height. Thus the total height of the cusp is

$$(2n-4) + (n-1) + 2 + (n-1) = 4n - 4.$$

(When $n = 2$ this argument needs to be modified slightly: there are no C_i's, but B_1 and B_2 are tangent. Tangencies of A and B_2, D and B_1, and A and D also contribute to the height. These all give 1 by 1 rectangles, and hence the height is $4 = 4n - 4$ in this case as well.)

A meridian runs along the widths of two rectangles in the cusp tiling. Hence it has length 2. Thus the normalized height $h(X)$ is given by:

$$h(X) = \frac{4n - 4}{\sqrt{(4n-4)(2)}} = \sqrt{2(n-1)}.$$

This information will show:

Proposition 6.8. *Let K be a 2–bridge knot in S^3 which admits a prime, twist reduced diagram with $n \geq 2$ twist regions and at least $c \geq 24$ crossings in each twist region. In a hyperbolic structure on $S^3 - K$, normalized such that the meridian has length 1, the height of the cusp of $S^3 - K$ satisfies:*

$$\left(\sqrt{2(n-1)} - \sqrt{n}(0.18456) \right)^2 \leq H \leq \left(\sqrt{2(n-1)} + \sqrt{n}(0.18456) \right)^2.$$

Proof. Let L be the augmented link corresponding to K. Provided we have at least $n \geq 2$ twist regions, Theorem 6.1 implies $S^3 - L$ is hyperbolic. We have seen in the above discussion that, provided we have at least $c \geq 24$ crossings in each twist region, the slope on each crossing circle of L on which we perform Dehn filling has normalized length at least $I(1.0)$. This implies that a cone deformation exists from $S^3 - L$

to $S^3 - K$ for which the tube radius is at least $R_1 = 1.0$ throughout. Then Theorem 1.4 implies the normalized height of the cusp of $S^3 - K$ satisfies:

$$-\frac{\sqrt{n}(2\pi)^2\sqrt{C(1.0)}}{(1 - e^{-2.0})} \leq h_\tau - \sqrt{2(n-1)} \leq \frac{\sqrt{n}(2\pi)^2\sqrt{C(1.0)}}{(1 - e^{-2.0})}.$$

Using the formulas for $C(1.0)$ from the proof of Lemma 4.3, we find

$$\sqrt{2(n-1)} - \sqrt{n}(0.18456) \leq h_\tau \leq \sqrt{2(n-1)} + \sqrt{n}(0.18456).$$

We obtain the final result by noting that if we scale such that the meridian has length 1, then the height is at least $(h_\tau)^2$. q.e.d.

References

[1] C.C. Adams, *Augmented alternating link complements are hyperbolic*, in 'Low-dimensional topology and Kleinian groups' (Coventry/Durham, 1984), London Math. Soc. Lecture Note Ser., **112**, Cambridge Univ. Press, Cambridge, 1986, 115–130, MR 0903861, Zbl 0632.57008.

[2] ———, *Waist size for cusps in hyperbolic 3-manifolds*, Topology **41**(**2**) (2002) 257–270, MR 1876890, Zbl 0985.57012.

[3] I. Agol, *Bounds on exceptional Dehn filling*, Geom. Topol. **4** (2000) 431–449, MR 1799796, Zbl 0959.57009.

[4] I. Agol, P.A. Storm, & W.P. Thurston, *Lower bounds on volumes of hyperbolic Haken 3-manifolds*, J. Amer. Math. Soc. **20**(**4**) (2007) 1053–1077, with an appendix by N. Dunfield, MR 2328715.

[5] K. Böröczky, *Packing of spheres in spaces of constant curvature*, Acta Math. Acad. Sci. Hungar. **32**(**3**–**4**) (1978) 243–261, MR 0512399, Zbl 0422.52011.

[6] J. Brock, K. Bromberg, R. Evans, & J. Souto, *Tameness on the boundary and Ahlfors' measure conjecture*, Publ. Math. Inst. Hautes Études Sci. **98** (2003) 145–166, MR 2031201, Zbl 1060.30054.

[7] J.F. Brock & K.W. Bromberg, *On the density of geometrically finite Kleinian groups*, Acta Math. **192**(**1**) (2004) 33–93, MR 2079598, Zbl 1055.57020.

[8] K. Bromberg, *Hyperbolic cone-manifolds, short geodesics, and Schwarzian derivatives*, J. Amer. Math. Soc. **17**(**4**) (2004) 783–826 (electronic), MR 2083468, Zbl 1061.30037.

[9] ———, *Rigidity of geometrically finite hyperbolic cone-manifolds*, Geom. Dedicata **105** (2004) 143–170, MR 2057249, Zbl 1057.53029.

[10] M. Eudave-Muñoz & J. Luecke, *Knots with bounded cusp volume yet large tunnel number*, J. Knot Theory Ramifications **8**(**4**) (1999) 437–446, MR 1697382, Zbl 0942.57005.

[11] D. Futer, E. Kalfagianni, & J.S. Purcell, *Dehn filling, volume, and the Jones polynomial*, J. Differential Geom. **78**(**3**) (2008) 429–464, MR 2396249.

[12] D. Futer & J.S. Purcell, *Links with no exceptional surgeries*, Comment. Math. Helv. **82**(**3**) (2007) 629–628, MR 2314056, Zbl 1134.57003.

[13] C.D. Hodgson & S.P. Kerckhoff, *Rigidity of hyperbolic cone-manifolds and hyperbolic Dehn surgery*, J. Differential Geom. **48**(**1**) (1998) 1–59, MR 1622600, Zbl 0919.57009.

[14] _____, *Universal bounds for hyperbolic Dehn surgery*, Ann. of Math. (2) **162**(**1**) (2005) 367–421, MR 2178964, Zbl 1087.57011.

[15] M. Lackenby, *Word hyperbolic Dehn surgery*, Invent. Math. **140**(**2**) (2000) 243–282, MR 1756996, Zbl 0947.57016.

[16] _____, *The volume of hyperbolic alternating link complements*, Proc. London Math. Soc. (3) **88**(**1**) (2004) 204–224, With an appendix by I. Agol and D. Thurston, MR 2018964, Zbl 1041.57002.

[17] O. Lehto, *Univalent functions and Teichmüller spaces*, Graduate Texts in Mathematics, **109**, Springer-Verlag, New York, 1987, MR 0867407, Zbl 0606.30001.

[18] W.B.R. Lickorish, *A representation of orientable combinatorial 3-manifolds*, Ann. of Math. (2) **76** (1962) 531–540, MR 0151948, Zbl 0106.37102.

[19] G.D. Mostow, *Strong rigidity of locally symmetric spaces*, Princeton University Press, Princeton, NJ, 1973, Annals of Mathematics Studies, **78**, MR 0385004, Zbl 0265.53039.

[20] G. Prasad, *Strong rigidity of **Q**-rank 1 lattices*, Invent. Math. **21** (1973) 255–286, MR 0385005, Zbl 0264.22009.

[21] J.S. Purcell, *Volumes of highly twisted knots and links*, Algebr. Geom. Topol. **7** (2007) 93–108, MR 2289805, Zbl 1135.57005.

[22] D. Rolfsen, *Knots and links*, Publish or Perish Inc., Berkeley, Calif., 1976, Mathematics Lecture Series, **7**, MR 0515288, Zbl 0339.55004.

[23] W.P. Thurston, *The geometry and topology of three-manifolds*, Princeton Univ. Math. Dept. Notes, 1979.

[24] _____, *Three-dimensional manifolds, Kleinian groups and hyperbolic geometry*, Bull. Amer. Math. Soc. (N.S.) **6**(**3**) (1982) 357–381, MR 648524, Zbl 0528.57009.

[25] A.H. Wallace, *Modifications and cobounding manifolds*, Canad. J. Math. **12** (1960) 503–528, MR 0125588, Zbl 0108.36101.

DEPARTMENT OF MATHEMATICS
BRIGHAM YOUNG UNIVERSITY, PROVO, UT 84602
and
MATHEMATICAL INSTITUTE
UNIVERSITY OF OXFORD
24-29 ST GILES', OXFORD, OX1 3LB, UK
E-mail address: jpurcell@math.byu.edu